Computational design of materials for nuclear reactors

Tonks, Michael R.; Andersson, Anders David Ragnar; Aitkaliyeva, Assel

To be published in: npj Computational Materials, Article 12, Vol. 1, iss. 106, 2026-02-05

DOI to publisher's version: 10.1038/s41524-026-01980-8

npj | computational materials

Review

Published in partnership with the Shanghai Institute of Ceramics of the Chinese Academy of Sciences

https://doi.org/10.1038/s41524-026-01980-8

Computational design of materials for nuclear reactors

Michael R. Tonks[1] ✉, David A. Andersson[2,3] & Assel Aitkaliyeva[1,3]

Computational design for fission reactor materials is ready to accelerate the development and qualification of nuclear materials. This review is primarily aimed at computational materials scientists that seek to apply ICME to the development of fission reactor materials. We summarize reactor materials and technology, discuss reactor material development and qualification today, show how ICME is being applied to the unique requirements of reactor materials, and provide a future vision.

As the world's appetite for electricity continues to grow exponentially, driven by global technological innovation and the proliferation of digital technologies, the demand for reliable, secure and economical energy sources of power with a high capacity factor (actual output divided by maximum output) has become increasingly pressing. Nuclear fission reactors, with their high energy density and extremely high capacity factor, have immense potential to meet the burgeoning energy needs of data centers and the broader technological landscape[1,2]. However, the development of materials capable of withstanding the extreme operating conditions encountered in various reactor technologies remains a critical challenge[3–5].

The harsh environments within nuclear fission reactors, including high temperatures, intense radiation fields, corrosive coolants, and complex thermomechanical stresses, can severely degrade the performance and useful life of materials used in fuel, structural components, and coolant systems[3–6]. New reactor technologies currently under development often have even more extreme conditions[4,6], making materials challenges even larger. In addition, reactor materials must perform not only during normal operation but also under rapid transients and design-basis accident conditions[7]. Overcoming these material-related challenges is essential to unlock the full potential of nuclear power and support the energy-intensive demands of technological development and modern computing.

Traditionally, the design and qualification of nuclear materials have relied heavily on extensive experimental testing and evaluation[8–10]. This approach, while robust, is time-consuming, resource-intensive, and incompatible with the rapid development and deployment required to meet the evolving needs of the nuclear industry[9,10]. To overcome the limitations of the traditional approach, computational design methodologies can be used as a complementary tool to accelerate the development, optimization, and qualification of materials[9,10].

Computational materials design techniques[11–15] and Integrated Computational Materials Engineering (ICME)[16–18], powered by advancements in high-performance computing, multiscale modeling, and data-driven methods, can greatly improve the understanding of material behavior under extreme conditions, predict performance, and guide the design of novel materials with improved properties. Incorporating these tools into the development and qualification of nuclear materials allows researchers to accelerate qualification, explore wider design spaces, identify promising candidates, and optimize performance, ultimately enabling more efficient and cost-effective reactor systems to meet the growing demands of the digital age[9,10,19].

This review article aims to provide an overview of the current state of computational design approaches for materials in nuclear fission reactors. Unlike past work focused on presenting similar visions to the nuclear community[9,19], here we focus on presenting the unique aspects of nuclear reactor materials to the computational materials community. We begin by summarizing the material requirements of the different components of a nuclear reactor in section "Reactor material types" and the key reactor technologies in section "Summary of nuclear reactor technologies", followed by a discussion of nuclear material qualification in section "Nuclear reactor material qualification in the US" and the traditional nuclear material design approach and its limitations in section "Traditional nuclear material design". In section "Integrated computational materials engineering for accelerated materials development" we then delve into the principles and applications of ICME. We discuss unique complications for ICME with nuclear materials and highlight specific examples where these techniques have been successfully applied to the development of materials for nuclear fission reactors in section "Applications of computational materials design to nuclear materials". Finally, in section "Future vision", we explore the future vision further integrating computational design into the nuclear materials landscape, paving the way for the next generation of advanced reactor systems that can power the technological advancements of the 21st century.

Reactor material types

Generally, a nuclear reactor generates electricity from heat using turbines much like coal or natural gas plants. The major difference is in how the heat is generated; in a nuclear reactor, the heat is generated by splitting fissile isotopes (isotopes that undergo fission when hit by low-energy neutrons)

[1]Materials Science and Engineering Department, University of Florida, Gainesville, FL, USA. [2]MST-8, Los Alamos National Laboratory, Los Alamos, NM, USA. [3]These authors contributed equally: David A. Andersson, Assel Aitkaliyeva. ✉e-mail: michael.tonks@ufl.edu

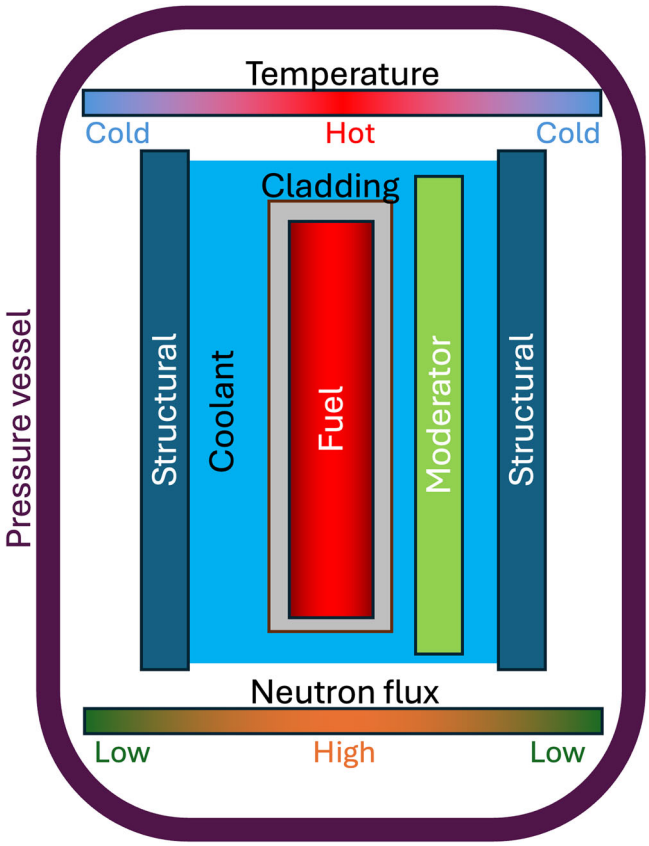

Fig. 1 | Schematic of the types of reactor materials. It shows general reactor positioning, interaction with coolant, and temperature and neutron flux ranges for the different types. Note that this figure also highlights the positioning of the material types as layers of defense against release of radioactive material from the fuel.

such as uranium-235 (235U), plutonium-239 (239Pu), and uranium-233 (233U). Once fission occurs, heat, gamma rays, and excess neutrons are released, and new elements are left behind, typically called fission products. The heat then has to be transported by the coolant to the turbines to generate electricity. For a nuclear reactor to complete these functions, various materials are needed, each with specific roles and unique operating conditions. These types of materials are summarized in the following subsections and in Fig. 1. Note that the figure highlights their relative temperature and neutron flux, but also the physical layers of defense preventing the release of radioactive material from the fuel. These layers reflect the safety functions that ultimately govern material requirements and qualification, and they shape why each material class must meet specific performance criteria under normal, transient, and accident conditions.

Fuel

The fuel material must contain fissile atoms and fission products, and sustain a controlled chain reaction. It must also withstand high-energy fission fragments and neutrons, as well as extreme temperatures and possible coolant interactions[20]. Efficient fuels should have a high fissile atom density, good thermal conductivity for heat transfer to the coolant, maintain dimensional stability under radiation damage, and have good chemical compatibility with the cladding.

The most widely used nuclear fuel worldwide is uranium dioxide (UO_2). However, UO_2 has some drawbacks in terms of efficiency, namely low thermal conductivity[21] and low uranium density[5]. Despite these limitations, UO_2 offers excellent safety characteristics: a stable crystal structure resistant to significant radiation damage, compatibility with water, and a high melting temperature[5,20,22]. Mixed oxide fuels, which contain both uranium and plutonium, are also used in some reactors and share similar properties with UO_2[5,23]. Metallic alloy fuels, such as uranium-zirconium (U-Zr)[24–26], uranium-plutonium-zirconium (U-Pu-Zr)[26], and uranium-molybdenum (U-Mo)[27,28], have been extensively used in test and demonstration reactors. Compared to UO_2, these alloys provide much higher thermal conductivity and uranium density, but lower melting temperatures and greater swelling. They are incompatible with water coolants, but can be used with liquid metals such as lead or sodium. Other uranium compounds have also been considered, including uranium carbides[29,30], oxycarbides[31–33], nitrides[34–36], silicides[37–39], borides[30], and hydrides[40]. These compounds typically offer higher thermal conductivity and uranium density than UO_2, as well as higher melting temperatures than uranium alloys. However, they often have less stable structures than UO_2 and react unfavorably with water-based coolants.

Coated particle fuels

Coated particle fuels, such as TRISO (Tristructural-Isotropic) fuel, have a unique composite structure that fills the roles of several reactor material types. They feature a multilayered coating around small fuel kernels, typically made of uranium oxycarbide (UCO) or UO_2[41]. The coatings, which include layers of pyrolytic carbon and silicon carbide, provide an additional barrier to the release of fission products and enhance the fuel's performance under high-temperature and radiation conditions. Coated particle fuels are designed to withstand extreme environments encountered in advanced reactor designs, such as high-temperature gas-cooled reactors (HTGRs) and do not require a separate cladding[41–43]. The primary benefit of these fuels is their safety due to excellent fission product retention even at very high temperatures, while their main weakness is their low uranium density since the fuel kernel is only a portion of the overall volume of the particle.

Coated particle fuels have been successfully employed in HTGRs and are being considered for implementation in other advanced reactor concepts[44], where their enhanced safety and performance characteristics can contribute to the overall reliability and efficiency of the nuclear power system. They are even being considered for use in LWRs[45]. There is also a topical report from the US Nuclear Regulatory Commission (NRC)[46] on the fuel, lowering the barrier to their use. The development of TRISO fuel is summarized section "TRISO particle development".

Cladding

The cladding material serves as a critical barrier between the fuel and the coolant. It prevents the fuel and fission products from escaping the fuel and entering the coolant, while also efficiently transferring heat from the fuel to the coolant. It must be able to withstand high temperatures, intense radiation fields, and potential chemical interactions with both the fuel and coolant. Ideal cladding materials should have low neutron absorption, good corrosion resistance, and sufficient mechanical strength to maintain fuel integrity under normal and accident conditions. Cladding is typically selected to match the fuel type. ensuring chemical and mechanical compatibility under reactor conditions.

The most widely used cladding materials in light water reactors (LWRs) are Zr-based alloys due to their low thermal neutron absorption cross section, good corrosion properties, and their compatibility with UO_2[47]. The development of Zr alloys for cladding is a good example of traditional nuclear material development and is summarized in section "Development of zirconium alloy cladding". However, Zr alloys have problems at the high temperatures that can occur during accidents: they can undergo rapid oxidation when exposed to steam or other oxidizing environments[48–50] and their mechanical properties can significantly degrade[51,52]. The development of accident-tolerant cladding materials, such as coated Zr alloys[53,54], iron-chromium-aluminum (FeCrAl) alloys[55–57] and silicon carbide (SiC) composites[58–60], is an ongoing effort. With fuel types other than UO_2, such as metallic fuels, stainless steels such as 316 or 304 have been used due to their good compatibility with metallic fuels, high-temperature strength, and reasonable resistance to liquid metal coolants like sodium[61,62]. However, their susceptibility to dimensional changes and hardening under irradiation makes them unattractive. Ferritic/martensitic steels, such as HT-9, are now

preferred for metallic fuels in fast reactors due to their greater radiation tolerance and improved high temperature properties[61–65].

Structural materials

Structural materials are used for various components within the reactor, such as the core internals, control rods, and other support structures. These materials must be able to withstand the high temperatures, intense radiation fields, and mechanical stresses present in the reactor environment. Ideal structural materials should possess high strength, good corrosion resistance, and sufficient radiation tolerance to maintain their integrity over reactor lifetime[6,66,67].

Common structural materials include stainless steels, nickel-based alloys, and advanced ferritic/martensitic steels. The specific composition and processing of these materials are tailored to optimize their performance in harsh reactor conditions, balancing factors such as mechanical properties, corrosion resistance, and radiation tolerance. This is especially important for advanced reactor designs that have harsher conditions than in LWRs[3,68–70]. Concrete[71,72] and graphite[73–75] are also used as structural materials in some reactor designs.

Pressure vessel material

The reactor pressure vessel (RPV) is a critical component for some reactors that contains the reactor core and coolant. It also serves as the ultimate barrier to the release of radioactive material. The RPV material must be able to withstand high pressures and temperatures, as well as the cumulative effects of radiation damage over reactor lifetime. The exact conditions vary depending on the type of reactor. Ideal RPV materials should exhibit high strength, toughness, and resistance to radiation embrittlement[76].

Typical RPV materials are low-alloy steels, with the specific composition and heat treatment optimized to provide the necessary mechanical properties and radiation resistance[77]. The development and testing of advanced RPV materials is ongoing, as engineers strive to enhance the safety and reliability of nuclear reactor designs[78–80].

Moderator materials

Moderator materials slow down fast neutrons produced during fission to thermal energies where the probability of further fission is much higher for 235U. For a material to be an effective moderator, it must be able to efficiently slow neutrons without significantly capturing them (high neutron scattering cross-section and a low neutron absorption cross-section)[81]. Moderator materials may be exposed to high temperatures, intense radiation fields, and direct contact with water, steam, or other coolants. Ideal moderators combine moderation effectiveness with resistance to radiation damage, dimensional and chemical stability under operational conditions, and minimal introduction of impurities or activation products to the reactor environment[82,83].

The most commonly used moderator materials are light water (ordinary H_2O), heavy water (D_2O)[84], graphite[74,85], and in some advanced concepts, beryllium[86] or zirconium hydride[82,87]. Graphite was historically used in early reactor designs and remains essential in some HTGRs due to its excellent moderation properties and high operating temperature tolerance.

Summary of nuclear reactor technologies

In the development of advanced materials for nuclear fission reactors, the context of the diverse range of reactor technologies currently in use or under development must be considered. Each reactor type presents unique operating conditions and material requirements that must be carefully addressed. Models and data for one reactor type are often not applicable to others due to their different conditions and materials. In this section, we provide a summary of the key reactor technologies and their associated materials challenges.

Light water reactors (LWRs)

LWRs, including pressurized water reactors and boiling water reactors, represent the dominant commercial nuclear power technology worldwide[88]. These reactors use light water as both coolant and moderator, operating at a temperature range of 300–350 °C[88]. All operating LWRs use UO_2 fuel and Zr-alloy cladding, though accident-tolerant cladding concepts, like FeCrAl[55] and SiC composites[58], and fuel concepts, like doped UO_2[89] and UN[35], are being considered. Major companies developing new LWR designs include GE Hitachi, NuScale, Westinghouse, Framatome, Holtec, EDF, and Rolls-Royce[90].

CANDU reactors

CANDU (CANada Deuterium Uranium) reactors form a significant class of commercial nuclear reactors that use D_2O as both moderator and coolant[91]. Their unique design features allow the use of natural uranium fuel without enrichment[92]. CANDU reactors typically operate at moderate temperatures (~300 °C), similar to LWRs, but have distinct material challenges due to D_2O chemistry and the use of pressure tubes instead of a large RPV. They use UO_2 fuel and Zr-alloy cladding, like LWRs. Material challenges include managing deuterium-induced corrosion and hydriding. The major producer and operator of CANDU reactors is Candu Energy (a division of SNC-Lavalin), and CANDU reactors are in service in Canada, South Korea, Romania, India (as PHWRs), and several other countries.

Metallic fuel fast reactors

Metallic fuel fast reactors (MFRs), such as sodium-cooled fast reactors (SFRs) or lead-cooled fast reactors (LFRs), utilize a fast neutron spectrum and metallic alloy fuels to achieve high breeding ratios and efficient fuel utilization[93,94]. These reactors operate at high temperatures (typically 400–550 °C) and employ liquid sodium or lead as the primary coolant, which presents unique materials challenges related to chemical compatibility, corrosion, and structural integrity[95]. The development of advanced fuel forms, cladding materials, and robust structural alloys is a critical area of research. Typical designs use U-Zr[24–26] or U-Pu-Zr[26] fuel with HT-9 cladding[61–65]. Because they operate with fast neutrons, a moderator is not required. TerraPower[96,97], Oklo, and ARC[98] are examples of companies developing SFRs.

Ceramic fuel fast reactors

Ceramic fuel fast reactors (CFRs), such as oxide-fueled sodium-cooled fast reactors (oxide SFRs) and lead-cooled fast reactors (oxide LFRs), use ceramic forms of nuclear fuel (e.g., UO_2, MOX, mixed actinide oxides, or UN) and operate with a fast neutron spectrum[99–101]. These reactors use liquid sodium or lead as coolant and operate at high temperatures (400–600 °C). The use of ceramic fuels offers greater chemical and dimensional stability at high temperatures and under irradiation compared to metallic fuels, but lower thermal conductivity and uranium density. Cladding materials must also resist attack by both the fuel and coolant; HT-9 is a common cladding material. Research focuses on advanced fuel forms such as minor-actinide-rich mixed oxides[102] and high-performance cladding[103]. Well-known designs include the BN-800 (Russia)[104,105] and ASTRID (France)[106–108].

High-temperature gas-cooled reactors (HTGRs)

HTGRs use helium as the primary coolant and operate at temperatures up to 700–950 °C[109,110]. These designs promise improved thermal efficiency and the possibility of supplying high-temperature process heat for applications such as hydrogen production. Materials must be capable of withstanding extreme temperatures, a chemically inert helium environment, and intense radiation[111]. Graphite compacts shaped as pellets or spheres containing TRISO particles are used as the fuel form[43]. Developers include China National Nuclear Corporation[112], X-Energy[113], General Atomics, and Japan Atomic Energy Agency[114,115].

Molten salt reactors (MSRs)

MSRs utilize a molten fluoride or chloride salt as coolant and, in some designs, as a solvent for the nuclear fuel[116,117]. They operate at elevated temperatures (typically 600–800 °C). The use of molten salt fuel allows for continuous refueling, efficient fission product removal, and elimination of

Table 1 | Summary of reactor technologies, showing the type, the coolant, the fuel material, the cladding material, and typical steady operating temperatures

Type	Coolant	Fuel	Cladding	Temperatures
LWR	H_2O	UO_2	Zr alloys	300–350 °C
CANDU	D_2O	UO_2	Zr alloys	300 °C
MFR	Liquid Na or Pb	U-Zr or U-Pu-Zr	HT-9	400–550 °C
CFR	Liquid Na or Pb	UO_2, MOX, or UN	HT-9	400–600 °C
HTGR	He gas	TRISO	N/A	700–950 °C
MSR	Molten salt	TRISO or Molten salt	N/A	600–800 °C

traditional radiation damage concerns. Molten salts offer high boiling points, low vapor pressures, and excellent heat transfer, but also introduce major challenges in terms of corrosion and structural performance[118,119]. Notable developers include Kairos Power (fluoride salt-cooled high-temperature reactor using TRISO fuel compacts)[120], Natura Resources (molten fluoride fuel and coolant), TerraPower (molten chloride fuel and coolant)[118], ThorCon (molten fluoride fuel and coolant)[121], Terrestrial Energy (molten fluoride fuel and coolant)[122], and Flibe Energy (molten fluoride fuel and coolant)[123].

Small modular reactors and microreactors

Small modular reactors (SMRs)[124–126] and microreactors[127–129] represent a new generation of compact, factory-fabricated nuclear power plants that offer enhanced safety, reduced capital cost, and deployment flexibility. These designs use a range of coolants, such as light water, gas, or molten salt, and thus inherit the material challenges described previously for each respective coolant type. However, there are also some unique components and challenges for each design, for example microreactors are often cooled with a heat pipe[130,131]. Materials must be tailored to the specific reactor concept and operating conditions, with a particular focus on safety, reliability, and manufacturability. Most new reactor designs under development are in the SMR or microreactor category.

Reactor operating conditions

The diverse range of nuclear fission reactor technologies, each with its unique normal operating conditions and material requirements (summarized in Table 1), presents a significant challenge in the development of advanced reactor materials. However, these materials also need to function in even more extreme conditions than the normal, steady operating conditions. They also need to maintain their required safety functions during transient and accident conditions.

Reactors are designed to experience three types of transient behavior[132]. Power transients are short-term, controlled departures from steady power, such as reactor startup or shutdown, power ramps, or load following (changing power during the day to follow power demand). The change in power results in changes in temperature, causing thermal stresses that can result in some fracture and fatigue without crossing into damage criteria if managed properly. Anticipated operational occurrences (AOOs) are disturbances expected to happen occasionally over a plant's life (e.g., a turbine trip or brief loss of feedwater). The reactor is designed to handle these automatically and return to a safe state without fuel damage or releasing radioactive material. Materials experience bounded, short-lived excursions in temperature, stress, and chemistry that the design accommodates. Design basis accidents (DBAs) are credible, low frequency "worst-case" events the plant is explicitly designed to withstand (e.g., large coolant pipe break, control rod ejection) and still keep the core cooled and radioactivity contained. Materials are assessed under extreme conditions (high temperatures, rapid cooling, elevated oxidation or embrittlement) against acceptance criteria that ensure cladding retains fission products, core structures maintain coolable geometry, and the pressure boundary remains intact.

The difficulty in testing materials in extreme reactor environments for the large lengths of time they will likely be in steady operation, as well as the short-term exposure to even more extreme transient conditions, is a large challenge. The need for materials capable of withstanding reactor-specific extreme environments while maintaining safety, reliability, and cost-effectiveness drives the growing use of computational materials design in the nuclear field. As these new reactor concepts are actively pursued, accelerating the development and qualification of suitable new materials is a critical priority for the nuclear industry.

Nuclear reactor material qualification in the US

In the US, the NRC governs which materials are used in safety-related reactor structures, systems, and components, primarily through Title 10 of the Code of Federal Regulations (CFR). The NRC also uses consensus codes and standards, like the American Society of Mechanical Engineers (ASME) Boiler and Pressure Vessel Code. Companion guidance covers ASME nuclear quality assurance (NQA-1), the assessment process for code verification, validation, and uncertainty quantification (V&V/UQ) in safety analyses, as well as environmental fatigue for new reactors and embrittlement correlations and surveillance. These regulations ensure that material behavior is acceptable during steady, transient, AOO, and DBA conditions.

Recent changes aim to create clearer, faster pathways to qualify new fuels and advanced structural materials without reducing safety margins. For fuels and cladding, the NRC has moved from zirconium-specific assumptions toward performance-based criteria and has supported staged deployment of accident-tolerant fuel via lead test rods and assemblies, plant-specific license amendments, and topical reports that establish generic methods and limits. For non-LWRs, the agency has endorsed a technology-inclusive, risk-informed, performance-based licensing framework that ties requirements to functions and risk significance rather than material pedigree, as outlined in NUREG-2246 for solid fuels[133] and NUREG/CR-7299 for molten salt technologies[134]. While these frameworks are independent and not cross-referencing; together they illustrate how the NRC is beginning to adapt, laying the groundwork for more flexible fuel qualification. Increased acceptance of mechanistic models to interpolate between accelerated testing and prototypical conditions is underway to make computational evidence a more integral part of the licensing basis[135]. This regulatory trajectory should favor performance-based demonstrations anchored by high-quality models linked directly to safety-relevant limits and degradation mechanisms.

Traditional nuclear material design

The traditional approach to designing and qualifying new materials for nuclear fission reactors has been predominantly empirical and experimental, as described by Crawford et al.[8], Karoutas et al.[47], and Terrani et al.[9] for fuel development, and Murty and Charit[68], Yvon and Carr´[69], and Chant and Murty[3] for structural material development. This methodology centers on comprehensive testing of candidate materials under realistic reactor conditions, including irradiation, mechanical loading, corrosion exposure, and other degradation mechanisms, to rigorously evaluate their performance and long-term suitability.

Historically, reactor material development followed an iterative, trial-and-error process. Researchers systematically varied composition, processing, and heat treatment, relying on repeated laboratory testing, in-reactor campaigns, and post-irradiation examinations[8,47]. Limited test reactor availability and the challenges of handling radioactive materials further complicated progress. As qualification requirements became more stringent, the time to develop new reactor materials increased significantly. Extended irradiation testing, lifetime performance data, accident scenario validation, and strict traceability requirements increased both time and cost. While general material development timeline is 10–20 years[136], nuclear material often require more than 25 years[8].

Although the empirical approach produced today's reactor materials, it was tightly coupled to a regulatory system that increasingly required prescriptive demonstrations. Since the late 1970s, NRC's reliance on

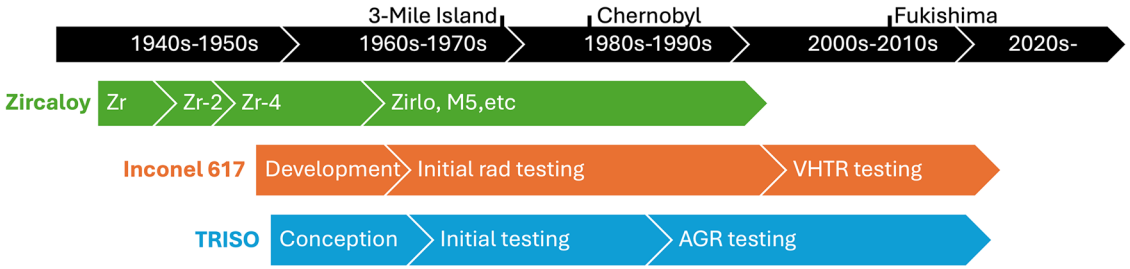

Fig. 2 | Development timelines for the example materials developed using the traditional approach. Timelines are shown for the development of Zr alloy cladding, Inconel 617, and TRISO fuel particles. Major reactor accidents are shown on the timeline to provide some context.

deterministic assumptions, extensive in-reactor data, and prescriptive code cases (for example, ASME's multi-decade effort to admit Alloy 617) has exposed the limitations of trial-and-error development. Recent shifts toward performance-based and technology-inclusive frameworks, as reflected in NUREG-2246 and NUREG/CR-7299, underscore the motivation for computationally guided design and accelerated qualification approaches. To illustrate the evolution, strengths, and weaknesses of traditional nuclear material development, we briefly review three representative examples: zirconium alloy cladding, Inconel 617, and TRISO fuel particles. Summarized development timelines for these materials are shown in Fig. 2.

Development of zirconium alloy cladding

The traditional material development approach prior to today's qualification frameworks is well exemplified by the development of Zr-based alloys for LWR cladding. Initial development in the late 1940s and 1950s[47,137] saw the selection of commercially pure Zr for its low neutron absorption, but at the cost of poor corrosion resistance. Metallurgists responded by empirically alloying Zr with tin (Sn), and later with small additions of Fe, Cr, and nickel (Ni), culminating in the introduction of the optimized Zircaloy-2 in the 1950s. This alloy, joined by Zircaloy-4 in the 1960s[138], dramatically improved corrosion resistance and mechanical integrity, facilitating longer fuel lifetimes and reliable operation in LWRs. Incremental improvements were made in the 1970s and 1980s, resulting in proprietary alloys such as ZIRLO[139] developed by Westinghouse, and M5[140] developed by Framatome.

Further advances in Zr alloys have proven far more challenging. Major accidents, notably Three Mile Island and Fukushima, exposed their vulnerability to high-temperature oxidation and hydrogen production in accident conditions. As a result, current development of so-called accident tolerant cladding, even those based on incremental chemistry changes or addition of coatings[141,142], face protracted, decade(s)-long qualification cycles involving extensive irradiation and accident testing.

Development and qualification of Inconel 617 for nuclear reactors

The development of Inconel 617 for high-temperature nuclear reactor applications offers another example of traditional nuclear materials. Inconel 617 is a wrought, nickel-chromium-cobalt-molybdenum alloy developed in the late 1960s[143,144]. Originally tailored for use in high-temperature petrochemical processing and gas turbine components, Alloy 617 combined exceptional strength[144], oxidation resistance, and stability at temperatures exceeding those of traditional stainless steels and earlier nickel-base alloys.

With the rise of interest in high-temperature reactor concepts like HTGRs during the 1970s and 1980s, Inconel 617 became a prime structural material candidate. Its suitability stemmed from its ability to maintain mechanical robustness and corrosion resistance in both high-temperature helium and impure process environments[143,144]. Early testing programs demonstrated Alloy 617's excellent thermal and irradiation stability up to temperatures of 950° C[143,145]. Laboratory mechanical and corrosion testing, along with in-reactor irradiation studies, built a substantial database and confidence in Alloy 617's performance[145]. However, it was not officially qualified for commercial nuclear deployment.

With renewed interest in high-temperature reactor systems in the 2000s, the process to formally qualify Alloy 617 for nuclear reactor components was revitalized. Comprehensive test campaigns, especially under the Generation IV Very High Temperature Reactor (VHTR) Materials Program, addressed critical questions on creep-rupture, long-term oxidation, weldability, and environmental effects[146,147]. These efforts culminated in 2019 with the successful ASME Boiler and Pressure Vessel Code approval of Alloy 617 for nuclear components operating at temperatures up to 950 °C, following more than four decades of incremental testing and code development.

TRISO particle development

The development trajectory of TRISO fuel particles provides another instructive example. Conceived in the 1960s[148,149], TRISO fuels were empirically optimized for HTGR and other advanced reactors[41]. Extensive international testing throughout the 1970s and 1980s (including operation in the US's Peach Bottom and Fort St. Vrain reactors, and in German programs) enabled improvement in fabrication methods, defect reduction, and fission product retention[41,42]. The German TRISO program was particularly influential, producing particles with low defect fractions and high coating quality, setting performance benchmarks that later U.S. development programs such as DOE Advanced Gas Reactor (AGR) program sought to match[42]. However, qualification standards demanded decades-long irradiation campaigns, post-irradiation examinations, and accident simulations, most notably under the AGR program in the 2000s–2010s[44]. Taken together, TRISO fuel development has spanned more than five decades, highlighting the long timelines inherent to traditional qualification. Only after meeting these requirements, did the NRC approve a topical report on AGR TRISO fuel[150]. While this was a major milestone, acceptance of a topical report does not itself constitute full fuel qualification for commercial use; rather, it establishes a reviewed body of data and methods that can be referenced in licensing for specific applications.

The NRC topical report underpins why advanced reactor developers now favor TRISO fuel: its qualification legacy circumvents the need for additional decades-long, high-cost development cycles. It is being considered for various reactor types beyond HTGRs[44], including MSRs[120], LWRs[45], microreactors[151,152], and even reactors for nuclear thermal propulsion in space[153]. TRISO particles are potentially over-designed for some of these other reactor applications but are being considered primarily to speed up qualification.

AGR TRISO is generally produced under stringent specifications, such as high kernel purity and low defect rates. While this quality underpinned the NRC's review, replicating it at scale, or with modest changes in kernel chemistry, would likely trigger new qualification campaigns. The challenge grows if recycled material is used as the uranium source for kernel fabrication, since isotopic composition and impurities can differ from AGR specifications; such differences would require new characterization and potentially additional qualification testing. This distinction is important: -œTRISO-refers to a class of designs, not a single fuel form, and AGR data are only directly applicable to AGR-quality TRISO produced to their specifications.

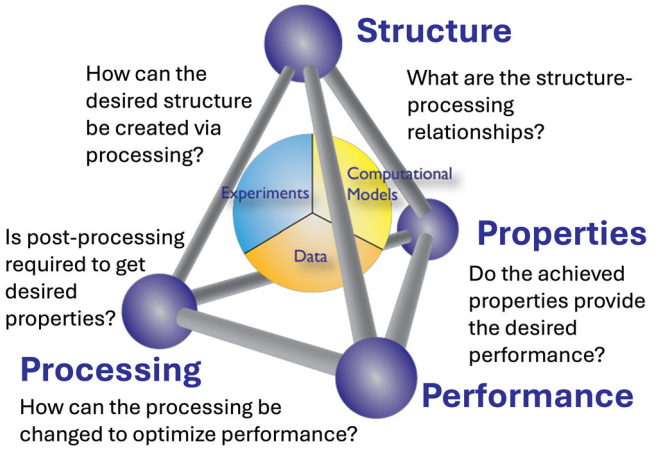

Fig. 3 | Materials tetrahedron driving ICME workflows. Questions that are answered during the ICME development process are included. The connections are made using data from modeling and simulation and experiments.

While TRISO fuels have the advantage of a rich qualification history, they also have notable drawbacks. For example, TRISO was not designed for recycling, and while recycling pathways are being explored, the economics are currently unfavorable: large fractions of fissile material remain unused at discharge[154], resulting in a larger disposal burden per unit of energy produced[155]. Furthermore, TRISO fabrication is an order of magnitude more expensive than conventional UO_2 fuel. Thus, it has significantly higher fuel cost per MWh. These drawbacks create an economic model that could be difficult to justify for wide-scale deployment outside HTGRs or MSRs.

Ultimately, TRISO's case illustrates how the perception of qualification advantage can overshadow considerations such as cost, waste generation, and reactor requirements. These lessons underscore the need for new paradigms in materials development and qualification, motivating the potential value of computational materials design.

Summary

Traditional nuclear material design has historically depended on a combination of empirical iteration and experimental validation. Materials developed before regulatory tightening in the late 1970s, such as Zircaloy cladding, benefited from relatively streamlined and pragmatic qualification pathways. In contrast, materials developed or modified since then face a much higher regulatory burden, with qualification cycles stretching to 20 years and beyond. This time and expense severely constrain the development of needed nuclear materials.

Integrated computational materials engineering for accelerated materials development

ICME is a modern approach that unifies materials science, engineering, and computational modeling in a systematic, iterative framework for the accelerated discovery, design, optimization, qualification, and deployment of new materials. Unlike the traditional method discussed in the previous section, ICME leverages multi-scale modeling, informatics, and high-throughput experimentation to predict how changes in materials and processing affect microstructure and properties, ultimately shortening development cycles and reducing cost and risk. In nuclear materials, where qualification alone can cost hundreds of millions of dollars and take decades, ICME offers a pathway to drastically compress timelines and reduce costs while maintaining safety margins. Here, we provide an overview of the ICME approach and then give examples of ICME success stories.

Overview of the ICME approach

ICME integrates computational models and experimental validation to enable the rapid design of materials and fabrication processes[16–18]. ICME builds on many years of development of computational materials capability, but was formally defined in 2008 in a US National Academies report[156]. The U.S. Materials Genome Initiative, launched in 2011, has been a major force in promoting ICME to speed discovery and reduce the average 10–20 year timeline traditionally required for new material deployment[136,157,158].

The core ICME philosophy is to replace expensive, slow, empirical testing with targeted, model-driven workflows that enable engineers to design from first principles for specific application requirements[16]. These workflows are organized around the concept of the materials tetrahedron, illustrating the connection in materials between the fabrication process, resultant structure, material properties, and the performance as summarized in Fig. 3. In ICME, detailed process-structure-property-performance relationships are constructed with a combination of multiscale modeling and high throughput experiments. By bridging atomistic, microscale, mesoscale, and macroscale phenomena, ICME enables a holistic understanding of how complex processing variables and microstructural features influence component-level behavior. This multiscale integration is essential for designing advanced materials with enhanced properties, optimizing manufacturing routes, tailoring performance for specific applications, and accelerating qualification and deployment to those applications. For nuclear materials, this means moving from decades of sequential irradiation campaigns to integrated model-experiment loops that can anticipate failure modes, optimize compositions, and justify performance within years rather than decades.

A typical ICME workflow begins with atomic-scale models such as density functional theory (DFT)[11,16] and molecular dynamics (MD)[16] that predict fundamental interactions, stability, and properties. These predictions inform mesoscale and continuum-scale simulations, including phase-field (PF) modeling[159,160], CALPHAD-based thermodynamic calculations[161], and computational mechanics[16,17], to connect microstructure evolution with macroscopic properties and in-service performance. Increasingly, data science and machine learning (ML) methods are being incorporated into ICME frameworks to accelerate materials exploration and optimize processing pathways, leveraging high-throughput simulations and large materials databases[18].

Despite its promise, ICME also faces challenges[158,162], especially in ensuring model fidelity across scales, integrating diverse types of data, and quantifying the uncertainties inherent in both simulation and experimentation[163]. Nevertheless, the growing adoption of ICME by industry and academia is enabling a new era of rational materials design, as illustrated by recent high-profile successes, described in the following subsections.

Ferrium S53, M54, and C64 steels for aerospace

A prominent ICME success story is the accelerated development of the Ferrium family of precipitation-strengthened steels (S53, M54, and C64) used in aerospace landing gear and transmission applications[164–166]. High-performance steels are critical for demanding aerospace applications, where components such as landing gear and transmission gears must combine exceptional strength, toughness, fatigue resistance, and corrosion resistance.

Northwestern University and QuesTek Innovations applied ICME to design the Ferrium S53, M54, and C64 alloys to address the needs of the aerospace industry[167,168]. Researchers leveraged CALPHAD thermodynamic modeling to explore multi-component alloy systems and accurately predict phase stability, precipitation behavior, and processability[169,170]. This modeling helped identify alloy compositions most likely to create fine, stable precipitates in a tough martensitic matrix, while minimizing detrimental phases. Kinetic simulations and property modeling detailed the influence of heat-treatment schedules, enabling virtual optimization of processing routes to further reduce experimental costs and time[164,167]. Experimental validation was tightly integrated throughout development, confirming predicted properties, resolving discrepancies, and refining both the alloy design and computational models[167]. These efforts resulted in the Ferrium S53 development taking 8.5 years[164,165] and M54 development just 6 years[171].

Ferrium S53, M54, and C64 have transitioned successfully from the laboratory to qualification and commercial release. S53 is available for

critical landing gear components in military and commercial aircraft[172], as is M54[173]. C64 is available for demanding gearbox and transmission applications[174]. The success of these alloys exemplifies the power of ICME: leveraging computational tools to accelerate development, tightly integrating modeling and experiment, and rapidly delivering transformational materials solutions that meet stringent real-world demands. This case also demonstrates how ICME can reduce development timelines from decades to under a decade, an acceleration highly relevant to nuclear materials.

Nickel-based alloy 718Plus (IN718+)

Alloy 718 (IN718), a nickel-based superalloy, has been a workhorse material in aerospace engines for decades due to its outstanding combination of strength, toughness, and processability. However, as NASA and industry partners pushed for higher engine efficiency and operating temperatures, IN718's temperature limit of 650 °C became a constraint. The need for a next-generation superalloy capable of retaining strength, manufacturability, and cost advantages up to 700 °C motivated the integrated development of IN718+ by ATI Allvac.

Using CALPHAD modeling, researchers rapidly explored the effects of minor alloying additions, boosting γ'-phase stability without causing the formation of detrimental phases[175]. Kinetic modeling predicted precipitation behavior and phase transformations during realistic thermal cycles, guiding the optimization of heat treatment procedures[176]. Experimental feedback cycles validated and refined model predictions[177]. This integrated design significantly reduced the typical development timeline for superalloys. Alloy IN718+ has been successfully qualified and deployed in next-generation turbine engine components, including disks, fasteners, and hot-section hardware, operating at temperatures up to 700 °C[178]. As with the Ferrium steels, the development of IN718+ highlights how ICME approaches can balance composition, processing, and performance requirements in a fraction of the traditional time, a lesson directly translatable to nuclear fuels and cladding.

Applications of computational materials design to nuclear materials

Just as the ICME approach is proving transformational in the development of new materials for more traditional applications, it can also transform the development of nuclear reactor materials. The use of materials informatics and multiscale modeling with integrated experimental validation and process modeling could enable an application-driven approach that will reduce the development time from 20 to 25 years to less than 10 years. This is similar to the approach suggested by Terrani et al.[9] and Aguiar et al.[19], which make similar claims of reduced development time. However, there are unique aspects of nuclear reactor materials that necessitate changes to the typical ICME framework. This work is already underway, though it is still early and no nuclear materials have yet completed development and qualification under an ICME paradigm. In this section, we first summarize the changes required in the ICME approach then review current ICME efforts that are already underway to model steady, transient, and accident behavior in the specific areas of reactor fuel, cladding, RPV material development, and additive manufacturing for reactor materials. We focus on these four areas as examples, but substantial modeling and simulation efforts are also ongoing in other nuclear materials domains, including radiation-tolerant structural alloys such as ODS steels, coolant compatibility with molten salts, and TRISO particle fuels.

Changes to the ICME approach

The harsh reactor environment during normal and accident conditions necessitates some changes to the standard ICME approach summarized in section "Integrated computational materials engineering for accelerated materials development". These changes include adding microstructure and chemistry evolution to the standard materials tetrahedron, expanding experimental validation to include separate-effects testing of extreme environments, and embedding qualification requirements (including V&V/UQ) directly into the development process.

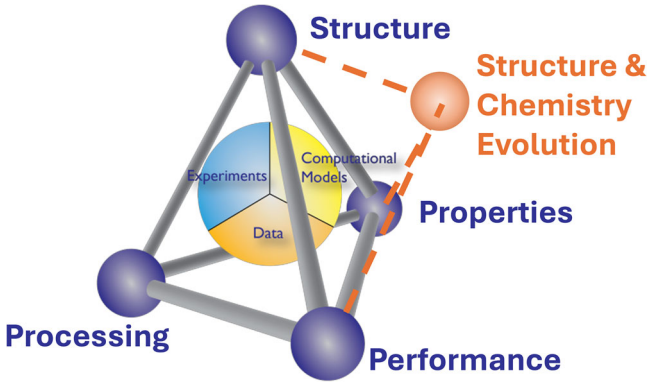

Fig. 4 | Modified materials tetrahedron for nuclear materials. It includes chemistry and microstructure evolution that occurs during reactor operation.

The standard ICME approach uses multiscale modeling to establish process-structure-property-performance relationships. These relationships enable the design of specific processing pathways that create a material microstructure that provides the necessary properties to ensure the required material performance for the application. However, in harsh reactor environments, the chemistry and microstructure evolves continuously over the reactor lifetime[179]. This evolution varies with the material and operating conditions: e.g., defect accumulation in structural materials, hydride formation in cladding, and fission product buildup in fuels. The evolution of the chemistry and microstructure drives changes in properties, which in turn alter performance. While such evolution occurs in other extreme environments, the scale and complexity in nuclear materials is unique. Thus, it is not enough to ensure acceptable initial performance; materials must maintain functionality during steady and transient operation. Because materials must meet acceptance criteria during AOOs and DBAs, not just steady operation, ICME workflows must explicitly model accident-condition behavior, including rapid temperature excursions, time-dependent degradation, and transient microstructure evolution that strongly influence safety margins.

Accordingly, when applying ICME to nuclear materials, the materials tetrahedron of process, structure, properties, and performance is not sufficient. A fifth aspect must be included: microstructure and chemical evolution during operation as shown in Fig. 4. This evolution must be explicitly considered across the ICME workflow. Multiscale modeling must therefore address not only initial structure-property relationships but also their time-dependent evolution. In fact, modeling this evolution has long been a focus of nuclear materials. Initially, empirical fits to experimental data were used to define changes in material properties with time, but more recently mechanistic models of chemistry and microstructure evolution and evolving properties have been developed for various materials[180]. Empirical models are specific to given materials and conditions that vary between reactor types, while mechanistic models are applicable as long as the fundamental mechanisms governing the behavior are the same and the specific material properties for the conditions are known.

The second change to the ICME approach is expanding validation through separate effects tests. Reactor environments combine multiple extremes: high temperature, radiation, stress, corrosive coolants, and rapid transients, yet very few facilities can expose materials to all extremes simultaneously, and such integral tests are rare, expensive, and time-consuming. While some integral test data are essential for model validation, data that includes separate effects or combinations of a few effects plays a critical role in accelerating and reducing the cost of validating nuclear material simulations[9,181]. In these tests, one or a subset of operating conditions is applied and material behavior is measured and/or characterized. For example, a material can be tested just at the operating temperature to observe the material behavior. The separate effect validation test is then simulated and the predicted behavior is compared to measured data.

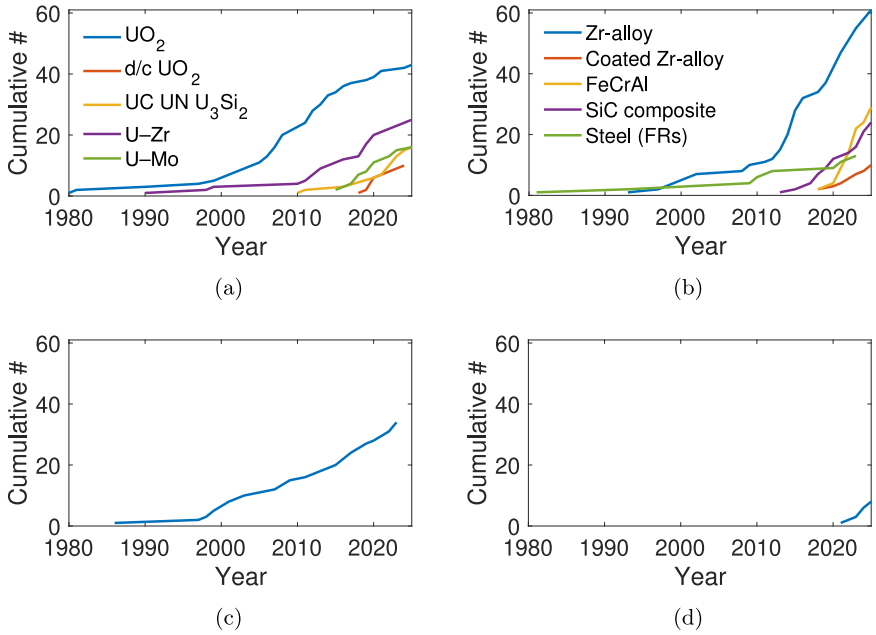

Fig. 5 | Cumulative number of papers cited in this work that present ICME approaches applied to nuclear material types. a is for fuel materials (with d/c UO_2 representing doped or composite UO_2), **b** for cladding materials, **c** for RPV steels, and **d** for AM applied to reactor materials. Note that these numbers only include work cited here and are not a comprehensive count of all modeling and simulation work related to these material types.

Multiple effects can also be included, in what are sometimes called "few effects tests", and again the validation test is simulated and the predicted behavior compared with the data. For example, a test can be carried out at high temperature with the sample exposed to the coolant. It is critical to conduct few effects testing to identify potential interactions between effects. The iterative application of separate and few effects tests and modeling and simulation must be a critical part of ICME for reactor materials, and should include much more than the comparison of data points. Simulation and experimental UQ need to be carried out so that uncertainty ranges are compared directly, and uncertainty is systematically reduced with each iteration.

Radiation testing merits special discussion. Structural, RPV, and cladding materials are all exposed to neutron radiation, while fuels are exposed to neutrons, gamma rays, and fission fragments. The only way to obtain neutrons for radiation testing is from nuclear reactors. However, test reactors are fairly rare and can be difficult and expensive to access. The radiation rates are also limited, requiring long times to reach high radiation dose. The time required for reactor testing for fuel development can be reduced with accelerated burnup testing[182] and using different neutron spectra[183]; combining these approaches with modeling and simulation can help to maximize its impact[183]. Other types of radiation can be used for separate effects radiation testing, including electron, ion, and proton radiation[184]. The most common tool is ion/proton irradiation, though ions/protons do not interact with materials in the same manner as neutrons; neutrons penetrate deeply and uniformly while ions/protons produce shallow damage layers, the PKA energy spectrum of ion/proton and neutron irradiation are different, and neutron's cause transmutation while ions/protons do not except at very high energy[185]. This results in challenges for using ion irradiation to emulate neutron damage. Even so, ion irradiation remains indispensable for nuclear materials development: it enables rapid, low-cost screening of compositions and microstructures, controlled single-variable testing, and access to extreme doses and temperatures that are impractical or impossible to achieve in test reactors. It can also be combined with neutron irradiation to accelerate the data collection required for material qualification, as presented by Taller et al.[186]. Finally, modeling and simulation can play a critical role in transitioning ion radiation data to predict material behavior under neutron radiation[187]. A validated model that accounts for radiation type can demonstrate how behavior observed in ion radiation experiments would differ under neutron exposure.

The third change needed in the ICME approach for nuclear materials arises from the rigorous qualification requirements for reactor deployment that ensure adequate performance during steady, transient, AOO, and DBA conditions. Since any new material must be qualified by the NRC or an NRC-approved agency such as ASME, these requirements should be embedded into the development process from the outset[187]. The qualification requirements are unavoidable and should be included in the ICME approach to accelerate eventual deployment. Therefore, the V&V/UQ standards required by the NRC should be applied to the full suite of multiscale modeling and simulation approaches applied to the system. Integration of V&V/UQ throughout the materials design process results in higher quality materials developed more quickly[163,188–191]. This also requires regulatory acceptance of modeling be more fully integrated into the qualification process[187]. At present, however, NRC guidance on V&V/UQ leaves room for interpretation, and there is still ambiguity in how different forms of uncertainty should be treated across scales and models. As a result, while modeling and simulation are increasingly accepted as complementary evidence, NRC is not yet prepared to rely on them in lieu of experimental data for material qualification.

ICME of reactor fuel

Here, we provide an overview of the application of ICME approaches to model nuclear reactor fuel. We start by highlighting a small fraction of the papers modeling UO_2 and then summarize the modeling efforts for other fuel types. In Fig. 5a we plot the cumulative number of papers we cite per their publication year for the various fuel types to provide a general timeline of the modeling efforts.

The properties[192–194] and macroscale performance[195] of UO_2 have been modeled for many years. Fuel performance models have been developed worldwide to predict the macroscale thermomechanical behavior of UO_2 during reactor operation[196–200]. MD simulations were first applied to UO_2 in the early 1980s[201], but were not widely applied until the 2000s[202–212]. Around 2010, the U.S. Department of Energy's Nuclear Energy Advanced Modeling and Simulation (NEAMS) program set out to replace empirical materials models for UO_2 used in LWR fuel performance codes with mechanistic models that capture the co-evolution of microstructure and properties[180]. The program adopted a multiscale strategy in which DFT and MD identified fundamental mechanisms and supplied key material parameters, while mesoscale PF simulations resolved microstructural evolution and its impact on effective properties. These physics-based results were distilled into

mechanistic constitutive models intended to supplant empirical correlations within engineering-scale fuel performance tools such as BISON[213,214], with validation against the extensive historical UO_2 database built over decades of fuel development.

From 2010 to 2020, NEAMS sponsored targeted modeling to clarify microstructure evolution in UO_2, including grain growth[215–217], defect transport[218–220], fission-gas bubble nucleation and growth[221–223], and recrystallization, as well as structure-property relationships for thermal conductivity[224–227], fracture strength[228–230], and creep[231,232]. These insights informed the development of mechanistic materials models for BISON[180]. While the net gain in code-level predictive accuracy was incremental, the work substantially deepened scientific understanding of UO_2 behavior and established a robust toolchain for modeling reactor fuel. The mechanistic modeling of UO_2 is now being extended to high burnup[233–239], as well as modeling transient and accident behavior such as fuel fracture, fragmentation, relocation, and dispersal[240–247] and transient fission gas release[248–250].

Beginning around 2015, these methods were generalized to accelerate development of advanced fuel forms. The first applications focused on doped UO_2, which exhibits accelerated sintering, larger as-fabricated grain sizes, improved fission-product retention, and better mechanical performance relative to standard UO_2[251]. DFT and MD clarified dopant-controlled defect chemistry and transport[252–254], feeding mesoscale simulations of sintering[255] and macroscale BISON analyses[256]. Atomistic studies identified a key mechanism for the improved behavior: an elevated concentration of negatively charged U vacancies induced by positively charged dopants[252]. This mechanism guided proposals for new dopants such as Mg and V[252] and culminated in a patent on Mg-doped UO_2[257]. The same multiscale approach has been applied to UO_2 composites to quantify conductivity gains from high-thermal-conductivity additives[258–260] and potential degradation via fission-gas segregation[261]. Uranium silicide has been explored for its higher uranium density and thermal conductivity relative to UO_2[262–264], balanced against concerns about its reactivity with water[265]. Uranium carbide modeling has emphasized atomistic treatments of bonding, defects, and thermodynamics[266–271]. Uranium mononitride has become a major focus, including interatomic potential development and assessment for MD[272,273], first-principles studies of fundamental behavior[274], defect diffusion[275,276], thermophysical properties[277], fabrication routes via CALPHAD[278], and integrated fuel performance projections[279]. Together, these efforts have laid the groundwork to move multiple fuel candidates more rapidly toward advanced reactor deployment.

In parallel, multiscale modeling of metallic fuels has progressed across U-Zr and U-Mo systems. System-level performance models for U-Zr date to the 1960s and continue to evolve[280–286]. Around 2010, atomistic studies of U-Zr addressed defects and diffusion[287–290] and phase stability[291–293], which informed mesoscale simulations of phase transformations[294–296] and, ultimately, macroscale constituent-redistribution models[297–299]. Thermal conductivity has been treated within multiscale frameworks[258,300–303], and fission-gas behavior has been quantified from first principles[304]. For U-Mo, work began with development of an interatomic potential[305] and atomistic studies of self- and defect diffusion[306–308], followed by mesoscale ICME treatments of fabrication and microstructure evolution[309–312]. Mesoscale models have also probed fission-gas behavior and its impact on conductivity[313–317], supported by additional atomistic inputs to refine fission-gas physics[318–321].

Thermodynamic descriptions spanning fresh and irradiated fuel have been extensively developed using CALPHAD. Accurate thermodynamics is essential for fresh fuels, which can exhibit multiple stable phases and non-stoichiometry[322], and becomes even more critical in-reactor to predict fission-product behavior and phase stability[323]. However, CALPHAD is fundamentally an equilibrium framework and needs to be coupled with other approaches such as cluster dynamics[324–326] or the PF method[223,298] to represent the non-equilibrium conditions that occur in reactor fuel. Given the breadth of this literature, we point to comprehensive reviews that synthesize progress across fuel chemistries and methods[322,327,328]. Thermodynamic models have been directly coupled to fuel performance solvers to improve treatment of evolving composition and phases[329,330]. The most complete database for nuclear fuel is the Thermodynamics of Advanced Fuels—International Database (TAF-ID)[331], developed by an international consortium.

ICME of cladding materials

As with fuel materials, ICME has been applied to cladding beginning with Zr alloys and steels for fast reactors. We begin by highlighting some of the modeling work focused on Zr alloys and then move on to other cladding materials. We provide a general timeline in Fig. 5b, showing the cumulative number of papers cited here for the various cladding materials.

Early atomistic simulations examined cascade damage in Zr[332,333], establishing baseline defect production and interaction energetics, though these studies were not yet used for alloy design. Subsequent atomistic work investigated iodine attack on Zr cladding[334–337], clarifying mechanistic pathways relevant to stress corrosion cracking. Atomistic modeling then expanded to defect transport, anisotropic point-defect energetics, and irradiation-induced growth[338–345]. Parallel atomistic and mesoscale efforts addressed oxidation, hydrogen pickup, and hydride formation. Atomic-scale studies focused on O and H behavior in the metal, oxides, and hydrides[346–353]. PF simulations have been used to capture oxide growth kinetics and stress coupling[354–358]. Because brittle hydrides are a major concern for cladding integrity, PF methods have been widely used to model hydride nucleation, growth, and morphology under stress and thermal gradients[359–378], although only two studies have targeted the transgranular hydrides most relevant to delayed hydride cracking[379,380]. Insights from experiments and lower-length-scale modeling have informed materials models in fuel performance codes[381,382]. Crystal plasticity has been used to probe anisotropic plasticity and texture effects[383–390] and to quantify irradiation growth and creep[391–393]. Thermodynamics databases for Zr alloys provide phase stability foundations for these models[394]. To date, however, most of this work has enhanced mechanistic understanding and code capabilities rather than directly driving new alloy chemistries or fabrication routes to improve Zircaloy behavior.

One accident-tolerant fuel (ATF) strategy retains Zr-alloy cladding but applies protective coatings such as Cr or FeCrAl to mitigate high-temperature steam oxidation. This concept remains under development and is therefore well-suited to ICME, yet modeling has largely focused on macroscale performance. Finite-element analyses and fuel-performance code studies have examined pellet-cladding mechanical interaction, stress redistribution, and failure margins in coated cladding in accident conditions[54,58,395–400]. Complementary continuum treatments have considered interdiffusion and coating integrity under reactor conditions[401,402]. At the lower length scales, crystal plasticity has recently been used to assess fatigue life in Cr-coated Zircaloy-4[403], providing microstructure-sensitive insights to inform coating design and qualification.

FeCrAl alloys are a second major ATF cladding candidate, and ICME has been applied across scales to assess and optimize their performance. Early macroscale thermo-mechanical simulations indicated that FeCrAl cladding can meet or exceed zircaloy performance under normal, transient, and accident conditions[404–409], with subsequent validation against new experimental data[410,411]. Composition optimization efforts have combined CALPHAD and ML to target protective oxide formation and mechanical robustness across operating and accident regimes[412–415]. At smaller scales, collision-cascade MD has characterized primary damage formation[416,417], and DFT, MD, discrete dislocation dynamics, and crystal plasticity have been used to connect defect physics to yield, hardening, and irradiation-assisted deformation in both unirradiated and irradiated states[418–425]. These insights are now propagating back into fuel-performance models to improve fidelity for FeCrAl cladding[426–428]. ML has also been used to relate precipitation to hardening across alloy variants[429]. On the environmental side, DFT studies of oxidation mechanisms are informing alloying strategies that promote resilient chromia/alumina scales[430–432], while PF modeling suggests irradiation-induced segregation and phase evolution pathways that

could influence hardening[433]. Collectively, this ICME workflow is accelerating FeCrAl cladding development.

SiC/SiC composite cladding is another prominent ATF concept, attractive for its oxidation resistance via protective silica formation and its low neutron absorption[434,435]. Macroscale models have evaluated mechanical and thermo-mechanical performance during steady, transient, and accident conditions and guided layer-architecture optimization[436–441], including requirements on effective composite thermal conductivity[442]. Composite behavior has been implemented in fuel-performance tools to capture fuel-cladding interactions[58], and mechanical damage models tailored to composite failure mechanisms have been developed[443,444]. Additional modeling has explored microstructural strategies, such as introducing bimodal porosity to relieve stress[445]. At the atomistic level, DFT has probed potential fuel-cladding interactions[446], and MD has addressed radiation response, swelling, and mechanical behavior[447–450]. Data-efficient ML has begun to predict swelling from sparse datasets[451]. Manufacturing-aware multiscale models are being used to simulate and optimize the braiding process[452,453]. Recognizing variability as a key risk, a probabilistic damage framework has been proposed for statistical performance assessment[454], and tribological models have examined wear of composite cladding tubes[455]. Given the complexity of SiC composites, coordinated multiscale initiatives are underway to support design and qualification for normal and accident conditions[456–458].

For fast reactors with liquid-metal coolants, steel claddings such as 316, 304, and HT-9 have been modeled primarily at the engineering scale. Fuel-performance frameworks with cladding materials models have been developed and refined over decades[459–466], supported by improved constitutive descriptions[467]. Crystal plasticity has provided mechanistic insight into deformation and creep[468], enabling data-driven surrogate constitutive models for HT-9 and 316 in fuel-performance codes[469,470]. Additional modeling has addressed corrosion by liquid metals[471] and predicted failure modes and mechanisms across designs[472].

ICME of reactor pressure vessel steels

Another example of ICME applied to nuclear reactor materials is the modeling of irradiation-induced hardening in RPV steels to support lifetime extension, and we show the cumulative number of papers cited in this work per publication year in Fig. 5c. This body of work has been heavily influenced by Dr. Robert Odette; ~40% of the papers summarized here involve him. The central mechanistic picture is that radiation-enhanced diffusion promotes the formation of nanoscale precipitates that impede dislocation motion and thereby harden and embrittle the steel matrix[80,473]. Early efforts developed semi-empirical and theoretical models grounded in hypothesized mechanisms and experimental trends[474–476], while fracture-mechanics-based approaches quantified failure behavior under irradiation-induced degradation[477–481].

These foundations enabled multiscale modeling and simulation frameworks that connect atomic-scale defect and precipitation processes to macroscopic property changes[482–485]. At the atomistic level, MD has been used to simulate displacement cascades and compared directly with positron annihilation measurements[486], while discrete dislocation dynamics informed by DFT has clarified the link between obstacle populations and hardening[487]. Interatomic potentials tailored for RPV chemistries have been developed to capture precipitation energetics[488], and MD has been applied to resolve precipitate evolution pathways[489]. Complementary atomic-scale Monte Carlo simulations elucidate phase formation and compositional partitioning under irradiation[489–491], while CALPHAD provides the thermodynamic basis for phase stability and driving forces[492,493].

Mesoscale and continuum models then translate these mechanisms to engineering-relevant predictions. PF simulations capture radiation-induced phase formation at dislocations and the emergence of distinctive core-shell precipitate morphologies[494–496]. Cluster dynamics models quantify defect and solute clustering kinetics under reactor fluxes and temperatures, enabling predictions of precipitate populations over service lifetimes[497–499]. Crystal plasticity links evolving microstructures to changes in macroscopic mechanical response and anisotropy[500]. In parallel, Monte Carlo strategies are being explored to assess thermal annealing as a mitigation pathway for embrittlement recovery[501], and extended finite element methods have been used to predict RPV cracking under thermal shock during accident transients[502]. Most recently, machine learning methods have emerged to accelerate embrittlement prediction by leveraging sparse, heterogeneous datasets and multiscale descriptors[503–505]. Collectively, this progression, from mechanistic models through atomistic, mesoscale, and continuum scales to data-driven surrogates, illustrates how ICME integrates physics and computation to produce predictive, transferrable tools for managing RPV steel performance over extended operating lifetimes.

ICME of additive manufacturing for reactor materials

Another critical facet of ICME is the explicit modeling of fabrication processes and their propagation through microstructure to in-service performance. The nuclear sector is beginning to explore novel manufacturing routes for safety-significant components, with additive manufacturing (AM) attracting attention for its ability to realize complex geometries, tailor local microstructures for corrosion and radiation tolerance, reduce feedstock waste, and speed iteration. At the same time, qualification concerns persist around part-to-part variability arising from localized heat input, scan strategy, and feedstock variability[506]. An ICME-centric response links process parameters to microstructure and properties via calibrated models, and wraps those models in digital twins that assimilate process monitoring and post-build characterization to forecast in-reactor performance[507]. In this framing, AM is not a black box but a controllable link in the digital chain, with UQ and targeted down-selection and testing used to close the loop where predictions most affect safety margins. Modeling and simulation is just beginning to be applied to AM for reactor materials, as shown in Fig. 5d.

Concretely, the MOOSE framework is being extended to nuclear AM, providing thermo-mechanical, microstructural, and performance modeling capabilities with embedded UQ[508,509], while machine learning accelerates surrogate model development and real-time inference[510]. ML has also been used to predict alloy printability in laser powder bed fusion, guiding composition/process choices upstream[511]. Downstream of the build, CALPHAD is informing post-AM heat-treatment windows, such as showing how annealing affects phase stability and properties in LPBF 709 austenitic stainless steel[512], and PF modeling is resolving irradiation-induced composition redistribution in AM austenitic Fe-Cr-Ni, with implications for hardening and corrosion resistance[513]. Together, these efforts exemplify process-aware ICME for AM: connecting build parameters to evolving microstructure and properties, quantifying uncertainty, and generating auditable models. Such integration is essential for the future qualification of AM parts for reactor service, where credible predictions, targeted separate-effects tests, and digital-chain traceability can de-risk deployment.

Future vision

The use of ICME approaches on nuclear materials has increased rapidly in the last 15 years, as shown in Fig. 5. With that foundation, the next decade should transform computational design for nuclear materials from a collection of compelling case studies into a repeatable, regulatory-aligned, and industry-scalable development pipeline. The guiding idea is a digital chain that links physics-based and data-driven models, targeted experiments, processing history, and qualification requirements to a living description of material behavior across its lifecycle, including handling at the end of life. This digital chain is a traceable, end-to-end linkage among data, models, assumptions, parameters, results, and decisions across the lifecycle, with machine-readable provenance, version control, persistent identifiers, and automated data exchange. Unlike traditional workflows that are file-centric and siloed (parameters are re-entered, assumptions are captured informally, and handoffs occur via ad hoc scripts and emails), the digital chain contains automated hand-offs where if new irradiation data become available, for example, the calibrated parameters would update, dependent simulations would rerun, and the change log would record the provenance and impact on predictions. If the traditional materials tetrahedron is expanded to

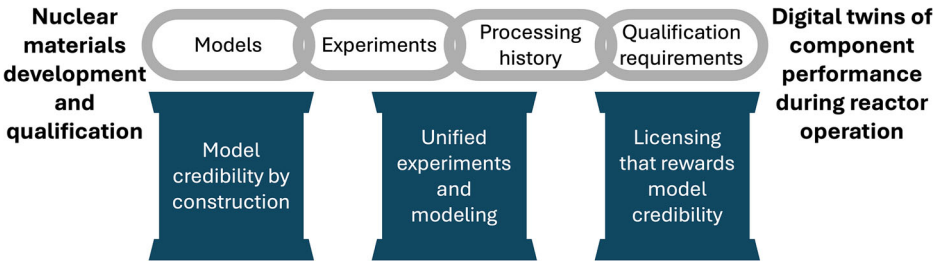

Fig. 6 | Summary of our future vision for ICME approaches applied to the design of nuclear reactor materials.

include chemistry and microstructure evolution, as argued earlier and shown in Fig. 4, this future ICME workflow must give that evolution and its uncertainties sufficient consideration in both design and licensing. This vision of the future is summarized in Fig. 6.

Three pillars are essential. First, models must be credible by construction. That means verification[294,329,514], validation[256,283,410], and uncertainty quantification[191,264,505,515–517] are included from the beginning, accuracy goals are tied to safety functions and acceptance criteria, and code quality control meets NRC quality expectations. Multi-fidelity strategies that combine mechanistic simulations (DFT, MD, PF, crystal plasticity, continuum mechanics) with surrogate models[469,470] and physics-informed machine learning[159,503,504] can provide the necessary accuracy-cost balance, but only if their domains of applicability, error bars, and failure modes are clear and explicit. This is especially important for multiscale modeling, where the model uncertainty from a lower length-scale simulation propagates through the predictions at a higher length scale[188,518], and so must be considered when quantifying its uncertainty. For actinide and complex alloy chemistries, the rapid maturation of machine-learned interatomic potentials[345,353] offers a path to first-principles accuracy in MD simulations, provided their training sets are curated, traceable, and stress-tested on independent benchmarks.

Second, experiments and multiscale modeling must be combined into a unified effort starting with the experimental design phase through qualification. Experimentalists and modelers should work together to design the full suite of experiments, ranging from separate effect, few effects, and integral reactor tests[163]. When modelers are directly included in the design of the separate effect and few effects tests, they help ensure that the necessary data on the conditions of the test are collected to allow them to use the data to validate their models. Then, the models validated on the separate and few effects tests can be used to assist in the design of the integral tests. As more in-situ measurement approaches become available in test reactors[519,520], the validated models can serve as digital twins[507,521–523] of the test, updating the predictions based on the in-situ data. Additional separate effects and few effects tests, designed by active learning and Bayesian optimal experimental design, should target the uncertainties that most influence safety margins and licensing decisions. High-throughput microstructural characterization and automated image analysis can turn postirradiation examination into quantitative datasets that close ICME loops, informing and validating models of microstructure evolution and its impact on properties.

Third, the licensing pathway should recognize and reward model credibility. Performance-based, risk-informed evidence packages that map model predictions and uncertainty to the Standard Review Plan's acceptance criteria can enable staged approvals. For example, method topical reports that establish the modeling framework and V&V/UQ pedigree could be approved. Then, early demonstrations via lead tests could be the basis for the next approval. Subsequent generic approvals would broaden use. For advanced reactors, technology-inclusive frameworks are a natural fit for material-agnostic performance criteria and for codes and standards that already accommodate high-temperature alloys, ceramics, and composites. Modeling and simulation will never eliminate the need for integral reactor testing but would enable targeted lead tests with maximized value for enabling approval, assuming NRC provides clear expectations. However, current NRC guidance does not clearly define how modeling evidence should be weighed against experimental data or what level of uncertainty is acceptable for licensing decisions, which limits how far ICME can be used today. A shared "materials licensing playbook" that aligns ICME artifacts with regulatory expectations would reduce friction for both applicants and reviewers.

Realizing this vision requires data infrastructure and community practice that make ICME reproducible and reusable. FAIR (findable, accessible, interoperable, and reusable) data standards, common formats for microstructure and property datasets, persistent identifiers for models and parameters, and machine-readable metadata describing training/validation domains will let others build on prior work rather than repeating it. Various nuclear materials experimental databases exist now[524–527], but their data are stored in different formats, and the available metadata are often incomplete or not provided. Irradiation conditions are typically documented, but microstructural datasets often lack essential metadata, such as sample preparation details, imaging conditions, calibration parameters (if any), and analysis methods. These vary significantly across laboratories, and even among individual researchers within the same laboratory, making it difficult to reuse data, compare results, or extract quantitative trends. Access to these databases varies widely, from open repositories to restricted archives that require applications, institutional sponsorship, data-use agreements, and adherence to proprietary or export-control rules. Open, curated nuclear materials benchmark problems that span atomistic to engineering scales, with reference datasets and scoring metrics, need to be developed to drive rapid, transparent progress and help separate model innovation from overfitting. The success of shared resources such as the TAF-ID[331] fuel thermodynamics database suggests analogous databases for other cladding and structural alloys, capturing both equilibrium and irradiation-modified thermodynamics and kinetics. Databases of defect properties are needed as well. We suggest that a shared platform be created that standardizes FAIR data standards and formats and encourages use in current and future databases, providing a common foundation for reproducible ICME, cross-laboratory comparability, and data structures suitable for modern computational and machine-learning methods.

In addition, manufacturing and variability must be pulled into the loop to extend the computational materials design approach from cradle to grave[19]. Process-aware ICME that couples thermo-mechanical processing, joining, coating deposition, and composite layup to microstructure and performance will shorten iteration cycles and surface trade-offs early. Probabilistic design, informed by variability in feedstock, process, and irradiation conditions, can translate microstructure distributions into property distributions and, ultimately, into uncertainty-informed safety margins. Surrogates and reduced-order models with quantified error will enable these probabilistic assessments to be used in design, surveillance, and operations. This design process should also be extended to the final handling of the used material.

Finally, the endpoint should be living digital twins[507,521–523] of critical components, such as fuel, cladding, and structural materials, during reactor operation that assimilate surveillance and operational data to update state and margin predictions over time. For LWRs, capsule surveillance and nondestructive evaluation can be fused with ICME models to inform aging management and life extension. For advanced reactors with embedded sensing, on-line state estimation can guide operations within material limits while generating data that improves the next design cycle. In this steady state, models no longer simply justify initial deployment; they help manage

materials throughout their life, providing a continuous feedback loop between design, qualification, operation, and final disposition.

Conclusion

This review shows that computational materials design and ICME are maturing to the point where they can accelerate nuclear materials development with a repeatable, auditable, and regulatory relevant pipeline. We have reviewed types of nuclear materials and the conditions faced by materials in different reactor types. We also reviewed the current approach for nuclear materials development and ICME. Treating in-service microstructure evolution as a core design variable, pairing targeted separate-effects experiments (with calibrated transfer to neutron conditions) to validate the models that matter most for safety margins, and embedding verification, validation, and uncertainty quantification under quality assurance are essential departures from standard ICME for nuclear reactor materials. Across fuels, cladding materials, and RPV steels, multiscale physics (DFT, MD, PF, crystal plasticity, CALPHAD, fuel-performance solvers) fused with physics-aware machine learning have produced mechanistic, multi-fidelity workflows that deepen understanding and yield predictive emulators, even though full qualification remains a work in progress.

To realize the promise of faster, lower-risk material development while preserving nuclear safety, we recommend building a digital chain that links processing, microstructure, properties, performance, and licensing artifacts; adopting FAIR data, community benchmarks, and persistent model metadata; and deploying multi-fidelity surrogates with explicit error bounds that feed staged, evidence-based licensing and living digital twins for surveillance and life-management. With coordinated investment in data infrastructure, integrated experimental-model campaigns, and early regulator engagement, these elements can compress development and qualification timelines, lower cost and program risk, and enable materials that meet the demanding performance and safety expectations of current and future reactor technologies.

Data availability

No datasets were generated or analyzed during the current study.

Received: 11 October 2025; Accepted: 25 January 2026;
Published online: 05 February 2026

References

1. Hanna, B. N., Abou-Jaoude, A., Guaita, N., Talbot, P. & Lohse, C. Navigating economies of scale and multiples for nuclear-powered data centers and other applications with high service availability needs. *Energies* **17**, 5073 (2024).
2. Soto Gonzalez, G. J. et al. *Powering Data Centers with Clean Energy: A Techno-economic Case Study of Nuclear And Renewable Energy Dependability*. Technical Report. (Idaho National Laboratory (INL), Idaho Falls, ID (United States) 2024).
3. Chant, I. & Murty, K. Structural materials issues for the next generation fission reactors. *JOM* **62**, 67–74 (2010).
4. Allen, T., Busby, J., Meyer, M. & Petti, D. Materials challenges for nuclear systems. *Mater. Today* **13**, 14–23 (2010).
5. Olander, D. Nuclear fuels–present and future. *J. Nucl. Mater.* **389**, 1–22 (2009).
6. Zinkle, S. J. & Busby, J. T. Structural materials for fission & fusion energy. *Mater. Today* **12**, 12–19 (2009).
7. Wachs, D. M. Transient testing of nuclear fuels and materials in the United States. *JOM* **64**, 1396–1402 (2012).
8. Crawford, D. C. et al. An approach to fuel development and qualification. *J. Nucl. Mater.* **371**, 232–242 (2007).
9. Terrani, K. A. et al. Accelerating nuclear fuel development and qualification: modeling and simulation integrated with separate-effects testing. *J. Nucl. Mater.* **539**, 152267 (2020).
10. Mika, M., Probert, A. & Aitkaliyeva, A. Nuclear fuel qualification: history, current state, and future. *Prog. Nucl. Energy* **177**, 105460 (2024).
11. Hafner, J., Wolverton, C. & Ceder, G. Toward computational materials design: the impact of density functional theory on materials research. *MRS Bull.* **31**, 659–668 (2006).
12. Kuehmann, C. J. & Olson, G. B. Computational materials design and engineering. *Mater. Sci. Technol.* **25**, 472–478 (2009).
13. Curtarolo, S. et al. The high-throughput highway to computational materials design. *Nat. Mater.* **12**, 191–201 (2013).
14. Butler, T. et al. Computational materials design of crystalline solids. *Chem. Soc. Rev.* **45**, 6138–6146 (2016).
15. Shevlin, S., Castro, B. & Li, X. Computational materials design. *Nat. Mater.* **20**, 727–727 (2021).
16. Horstemeyer, M. F. *Integrated Computational Materials Engineering (ICME) for Metals: Concepts and Case Studies* (John Wiley & Sons, 2018). Google-Books-ID: OkJLDwAAQBAJ.
17. Ghosh, S., Woodward, C. & Przybyla, C. *Integrated Computational Materials Engineering (ICME): Advancing Computational and Experimental Methods* (Springer Nature, 2020). Google-Books-ID: Xi3YDwAAQBAJ.
18. Wang, W. Y. et al. A brief review of data-driven ICME for intelligently discovering advanced structural metal materials: Insight into atomic and electronic building blocks. *J. Mater. Res.* **35**, 872–889 (2020).
19. Aguiar, J. A., Jokisaari, A. M., Kerr, M. & Allen Roach, R. Bringing nuclear materials discovery and qualification into the 21st century. *Nat. Commun.* **11**, 2556 (2020).
20. *Fundamental Aspects of Nuclear Reactor Fuel Elements: Solutions to Problems*. Technical Report. (Department of Nuclear Engineering, California University, Berkeley (USA), 1976).
21. Fink, J. K. Thermophysical properties of uranium dioxide. *J. Nucl. Mater.* **279**, 1–18 (2000).
22. Manara, D. et al. Thermodynamic and thermophysical properties of the actinide carbides (2012).
23. Parrish, R. & Aitkaliyeva, A. A review of microstructural features in fast reactor mixed oxide fuels. *J. Nucl. Mater.* **510**, 644–660 (2018).
24. Gaiduchenko, A. B. Thermophysical properties of irradiated uranium-zirconium fuel. *Energy* **104**, 5–10 (2008).
25. Ahn, S., Irukuvarghula, S. & McDeavitt, S. M. Thermophysical investigations of the uranium-zirconium alloy system. *J. Alloy. Compd.* **611**, 355–362 (2014).
26. Janney, D. E. et al. *Metallic Fuels Handbook*. Technical Report. (Idaho National Lab. (INL), Idaho Falls, ID (United States), 2017).
27. Meyer, M. K. et al. Low-temperature irradiation behavior of uranium-molybdenum alloy dispersion fuel. *J. Nucl. Mater.* **304**, 221–236 (2002).
28. Ajantiwalay, T., Smith, C., Keiser, D. D. & Aitkaliyeva, A. A critical review of the microstructure of U-Mo fuels. *J. Nucl. Mater.* **540**, 152386 (2020).
29. Vasudevamurthy, G. & Nelson, A. T. Uranium carbide properties for advanced fuel modeling—a review. *J. Nucl. Mater.* **558**, 153145 (2022).
30. Watkins, J. K., Wagner, A. R., Gonzales, A., Jaques, B. J. & Sooby, E. S. Challenges and opportunities to alloyed and composite fuel architectures to mitigate high uranium density fuel oxidation: uranium diboride and uranium carbide. *J. Nucl. Mater.* **560**, 153502 (2022).
31. Chiotti, P., Robinson, W. C. & Kanno, M. Thermodynamic properties of uranium oxycarbides. *J. Less Common Met.* **10**, 273–289 (1966).
32. Phillips, J. A., Nagley, S. G. & Shaber, E. L. Fabrication of uranium oxycarbide kernels and compacts for HTR fuel. *Nucl. Eng. Des.* **251**, 261–281 (2012).
33. Wojtaszek, D. T. & Bromley, B. P. Physics evaluation of alternative uranium-based oxy-carbide annular fuel concepts for potential use

in compact high-temperature gas-cooled reactors. *J. Nucl. Eng. Rad. Sci*. **9**, 011504 (2023).
34. Watkins, J. K., Gonzales, A., Wagner, A. R., Sooby, E. S. & Jaques, B. J. Challenges and opportunities to alloyed and composite fuel architectures to mitigate high uranium density fuel oxidation: uranium mononitride. *J. Nucl. Mater.* **553**, 153048 (2021).
35. Sajdova, A. *Accident-Tolerant Uranium Nitride*. PhD Thesis, Chalmers University of Technology (2017).
36. Hania, P. R. et al. Irradiation and post-irradiation examination of uranium-free nitride fuel. *J. Nucl. Mater.* **466**, 597–605 (2015).
37. Birtcher, R. & Wang, L. Stability of uranium silicides during high energy ion irradiation. *MRS Online Proc. Libr.* **235**, 467 (1991).
38. Finlay, M. R., Hofman, G. L. & Snelgrove, J. L. Irradiation behaviour of uranium silicide compounds. *J. Nucl. Mater.* **325**, 118–128 (2004).
39. Gonzales, A., Watkins, J. K., Wagner, A. R., Jaques, B. J. & Sooby, E. S. Challenges and opportunities to alloyed and composite fuel architectures to mitigate high uranium density fuel oxidation: uranium silicide. *J. Nucl. Mater.* **553**, 153026 (2021).
40. Greenspan, E. et al. Hydride fuel for LWRs—project overview. *Nucl. Eng. Des.* **239**, 1374–1405 (2009).
41. Demkowicz, P. A., Liu, B. & Hunn, J. D. Coated particle fuel: historical perspectives and current progress. *J. Nucl. Mater.* **515**, 434–450 (2019).
42. Petti, D. A., Buongiorno, J., Maki, J. T., Hobbins, R. R. & Miller, G. K. Key differences in the fabrication, irradiation and high temperature accident testing of US and German TRISO-coated particle fuel, and their implications on fuel performance. *Nucl. Eng. Des.* **222**, 281–297 (2003).
43. Zhou, X. W. & Tang, C. H. Current status and future development of coated fuel particles for high temperature gas-cooled reactors. *Prog. Nucl. Energy* **53**, 182–188 (2011).
44. Brown, N. R. A review of in-pile fuel safety tests of TRISO fuel forms and future testing opportunities in non-HTGR applications. *J. Nucl. Mater.* **534**, 152139 (2020).
45. Brown, N. R., Hernandez, R. & Nelson, A. T. High volume packing fraction TRISO-based fuel in light water reactors. *Prog. Nucl. Energy* **146**, 104151 (2022).
46. Petti, D. A. *NGNP Fuel Qualification White Paper.* Technical Report. (Idaho National Lab (INL), Idaho Falls, ID (United States), 2010).
47. Karoutas, Z. et al. The maturing of nuclear fuel: past to accident tolerant fuel. *Prog. Nucl. Energy* **102**, 68–78 (2018).
48. Chapman, R., Crowley, J., Longest, A. & Hofmann, G. *Zircaloy Cladding Deformation in a Steam Environment with Transient Heating*. Technical Report. (Oak Ridge National Lab., TN (USA), 1978).
49. Moalem, M. & Olander, D. R. Oxidation of Zircaloy by steam. *J. Nucl. Mater.* **182**, 170–194 (1991).
50. Kim, H. H. et al. High-temperature oxidation behavior of Zircaloy-4 and Zirlo in steam ambient. *J. Mater. Sci. Technol.* **26**, 827–832 (2010).
51. Hayes, T. A. & Kassner, M. E. Creep of zirconium and zirconium alloys. *Metall. Mater. Trans. A* **37**, 2389–2396 (2006).
52. Massih, A. High-temperature creep and superplasticity in zirconium alloys. *J. Nucl. Sci. Technol.* **50**, 21–34 (2013).
53. Kim, H.-G. et al. Adhesion property and high-temperature oxidation behavior of cr-coated zircaloy-4 cladding tube prepared by 3d laser coating. *J. Nucl. Mater.* **465**, 531–539 (2015).
54. Lee, Y., Lee, J. I. & No, H. C. Mechanical analysis of surface-coated zircaloy cladding. *Nucl. Eng. Technol.* **49**, 1031–1043 (2017).
55. Rebak, R. B. Iron-chrome-aluminum alloy cladding for increasing safety in nuclear power plants. *EPJ Nucl. Sci. Technol.* **3**, 34 (2017).
56. Charit, I. Accident tolerant nuclear fuels and cladding materials. *JOM* **70**, 173–175 (2018).
57. Yin, L. et al. Uniform corrosion of FeCrAl cladding tubing for accident tolerant fuels in light water reactors. *J. Nucl. Mater.* **554**, 153090 (2021).
58. Wagih, M., Spencer, B., Hales, J. & Shirvan, K. Fuel performance of chromium-coated zirconium alloy and silicon carbide accident tolerant fuel claddings. *Ann. Nucl. Energy* **120**, 304–318 (2018).
59. Braun, J. et al. Chemical compatibility between UO2 fuel and SiC cladding for LWRs. Application to ATF (Accident-Tolerant Fuels). *J. Nucl. Mater.* **487**, 380–395 (2017).
60. Pham, H. V., Kurata, M. & Steinbrueck, M. Steam oxidation of silicon carbide at high temperatures for the application as accident tolerant fuel cladding, an overview. *Thermo* **1**, 151–167 (2021).
61. Azevedo, C. R. F. A review on neutron-irradiation-induced hardening of metallic components. *Eng. Fail. Anal.* **18**, 1921–1942 (2011).
62. Allen, T., Burlet, H., Nanstad, R. K., Samaras, M. & Ukai, S. Advanced structural materials and cladding. *MRS Bull.* **34**, 20–27 (2009).
63. Keiser, D. D. *3.15-Metal Fuel-Cladding Interaction* (Elsevier, 2012).
64. Was, I. & Beam, H. F. I. 3.3 Advanced Reactor Cladding. *Advanced Fuels Campaign Fy 2015 Accomplishments Report* 96 (2015).
65. Sencer, B. H., Kennedy, J. R., Cole, J. I., Maloy, S. A. & Garner, F. A. Microstructural stability of an HT-9 fuel assembly duct irradiated in FFTF. *J. Nucl. Mater.* **414**, 237–242 (2011).
66. Roberts, J. T. A. *Structural Materials in Nuclear Power Systems* (Springer Science & Business Media, 2013). Google-Books-ID: 36jhBwAAQBAJ.
67. Yvon, P., Le Flem, M., Cabet, C. & Seran, J. L. Structural materials for next generation nuclear systems: challenges and the path forward. *Nucl. Eng. Des.* **294**, 161–169 (2015).
68. Murty, K. L. & Charit, I. Structural materials for Gen-IV nuclear reactors: challenges and opportunities. *J. Nucl. Mater.* **383**, 189–195 (2008).
69. Yvon, P. & Carré, F. Structural materials challenges for advanced reactor systems. *J. Nucl. Mater.* **385**, 217–222 (2009).
70. Yvon, P. *Structural Materials for Generation IV Nuclear Reactors* (Woodhead Publishing, 2016). Google-Books-ID: i3W0CwAAQBAJ.
71. Pomaro, B. A review on radiation damage in concrete for nuclear facilities: from experiments to modeling. *Model. Simul. Eng.* **2016**, 4165746 (2016).
72. Kurtis, K. E. et al. Can we design concrete to survive nuclear environments. *Concr. Int* **39**, 53–59 (2017).
73. Marsden, B., Jones, A., Hall, G., Treifi, M. & Mummery, P. *Graphite as a Core Material for Generation IV Nuclear Reactors* (Elsevier, 2017).
74. Zhou, X. -w, Tang, Y. -p, Lu, Z. -m, Zhang, J. & Liu, B. Nuclear graphite for high temperature gas-cooled reactors. *New Carbon Mater.* **32**, 193–204 (2017).
75. Kurpaska, L. et al. Structural and mechanical properties of different types of graphite used in nuclear applications. *J. Mol. Struct.* **1217**, 128370 (2020).
76. Zhou, L. et al. Research progress of steels for nuclear reactor pressure vessels. *Materials* **15**, 8761 (2022).
77. Davies, L. M. A comparison of Western and Eastern nuclear reactor pressure vessel steels. *Int. J. Press. Vessels Pip.* **76**, 163–208 (1999).
78. Phythian, W. J. & English, C. A. Microstructural evolution in reactor pressure vessel steels. *J. Nucl. Mater.* **205**, 162–177 (1993).
79. Odette, G. R. Radiation induced microstructural evolution in reactor pressure vessel steels. *MRS Online Proc. Libr.* **373**, 137 (1994).
80. Odette, G. R. & Lucas, G. E. Recent progress in understanding reactor pressure vessel steel embrittlement. *Radiat. Eff. Defects Solids* **144**, 189–231 (1998).
81. Shivprasad, A. P. et al. *Advanced Moderator Material Handbook*. Technical Report. (LA-UR-20-27683, Los Alamos National Laboratory (LANL), Los Alamos, NM (United States), https://doi.org/10.2172/1671020. https://www.osti.gov/biblio/1671020 (2020).
82. Vetrano, J. B. Hydrides as neutron moderator and reflector materials. *Nucl. Eng. Des.* **14**, 390–412 (1971).

83. Gustafson, J. L. Space nuclear propulsion fuel and moderator development plan conceptual testing reference design. *Nucl. Technol.* **0**, 1–3 (2021).
84. Cameron, I. R. The heavy-water-moderated reactor. in *Nuclear Fission Reactors* (ed Cameron, I. R.) 269–282 (Springer US, 1982).
85. Baker, D. E. Graphite as a neutron moderator and reflector material. *Nucl. Eng. Des.* **14**, 413–444 (1971).
86. Beeston, J. M. Beryllium metal as a neutron moderator and reflector material. *Nucl. Eng. Des.* **14**, 445–474 (1971).
87. Miao, Y., Stauff, N., Bhattacharya, S., Yacout, A. & Kim, T. K. *Advanced Moderation Module for High-Temperature Micro-Reactor Applications*. Technical Report. (ANL/CFCT-20/19, Argonne National Lab. (ANL), Argonne, IL (United States), https://doi.org/10.2172/1656612. https://www.osti.gov/biblio/1656612 (2020).
88. Ehrlich, K., Konys, J. & Heikinheimo, L. Materials for high performance light water reactors. *J. Nucl. Mater.* **327**, 140–147 (2004).
89. Terricabras, A. J. et al. Performance and properties evolution of near-term accident tolerant fuel: Cr-doped uo2. *J. Nucl. Mater.* **594**, 155022 (2024).
90. Pieńkowski, L. Competitiveness strategies and technical innovations in light-water small modular reactor projects. *Energies* **18**, 1268 (2025).
91. Pasanen, A. A. Fundamentals of CANDU reactor nuclear design. 131–214. https://inis.iaea.org/records/e866m-7kj92 (1982).
92. Morad, C. M., Stefani, G. L. d., Santos, T. A. d. & Associação Brasileira de Energia Nuclear (ABEN), R. d. J. *CANDU: Study and Review*. Technical Report. (INIS-BR–19726, Associação Brasileira de Energia Nuclear (ABEN), Rio de Janeiro, RJ (Brazil) https://inis.iaea.org/records/j1qfj-fpw08 (2017).
93. Lineberry, M. J. & Allen, T. R. *The Sodium-Cooled Fast Reactor (SFR)*. Technical Report. (ANL/NT/CP-108933, Argonne National Lab., IL (US) https://www.osti.gov/biblio/803901 (2002).
94. Ohshima, H. & Kubo, S. 5 - Sodium-cooled fast reactor. In *Handbook of Generation IV Nuclear Reactors* (ed Pioro, I. L.) Woodhead Publishing Series in Energy, 97–118 (Woodhead Publishing, 2016).
95. Aoto, K. et al. A summary of sodium-cooled fast reactor development. *Prog. Nucl. Energy* **77**, 247–265 (2014).
96. The Natrium technology: Providing reliable, carbon-free energy to complement wind and solar.
97. Natrium™ Reactor and Integrated Energy Storage. https://www.ans.org/news/article-2782/the-natrium-technology-providing-reliable-carbonfree-energy-to-complement-wind-and-solar/ (2022).
98. McTiernan, N. Arc-100 sodium fast reactor pressure boundary classification and material selection. In *Proc. Canadian Nuclear Society* (2023).
99. Kittel, J. H. et al. History of fast reactor fuel development. *J. Nucl. Mater.* **204**, 1–13 (1993).
100. Burkes, D. E., Fielding, R. S., Porter, D. L., Meyer, M. K. & Makenas, B. J. A US perspective on fast reactor fuel fabrication technology and experience. Part II: Ceramic fuels. *J. Nucl. Mater.* **393**, 1–11 (2009).
101. Raj, B., Vasudeva Rao, P., Puthiyavinayagam, P. & Ananthasivan, K. Advanced ceramic fuels for sodium-cooled fast reactors. *Handbook of Advanced Ceramics and Composites: Defense, Security, Aerospace and Energy Applications* 667–702 (Springer, 2020).
102. Sommer, C. M. et al. Transmutation fuel cycle analyses of the SABR fission-fusion hybrid burner reactor for transuranic and minor actinide fuels. *Nucl. Technol.* **182**, 274–285 (2013).
103. Kataeva, N. et al. Comparative analysis of the long-term strength of russian ferritic-martensitic reactor steels. *J. Nucl. Mater.* **605**, 155575 (2025).
104. Saraev, O. M. et al. BN-800 design validation and construction status. *Energy* **108**, 248–253 (2010).
105. Tashlykov, O. L., Sesekin, A. N., Klimova, V. A. & Mahmoud, K. A. Optimization of the route of the refueling machine to reduce the refueling time: Case study of the BN-800 reactor. *Nucl. Eng. Des.* **431**, 113725 (2025).
106. Coz, P. L., Sauvage, J.-F. & Serpantie, J.-P. Sodium-Cooled Fast Reactors: the ASTRID Plant Project. Revue Générale Nucléaire 39–44. https://doi.org/10.1051/rgn/20115039 (2011).
107. Chanteclair, F., Rodriguez, G., Hamy, J.-M. & Dupraz, R.ASTRID reactor: design overview and main innovative options for Basic Design. https://cea.hal.science/cea-02435077 (2017).
108. Varaine, F. et al. The collaboration of Japan and France on the design of Astrid sodium fast reactor. In *International Congress on Advances in Nuclear Power Plants (ICAPP - 2017)* (International Congress on Advances in Nuclear Power Plants (ICAPP—2017), 2017).
109. Goodjohn, A. J. Summary of gas-cooled reactor programs. *Energy* **16**, 79–106 (1991).
110. Iwatsuki, J. et al. 1 - Overview of high temperature gas-cooled reactor. In Takeda, T. & Inagaki, Y. (eds.) *High Temperature Gas-Cooled Reactors*, Vol. 5 of JSME Series in Thermal and Nuclear Power Generation 1–16 (Academic Press, 2021).
111. Beck, J. M. & Pincock, L. F. *High Temperature Gas-Cooled Reactors Lessons Learned Applicable to the Next Generation Nuclear Plant*. Technical Report. INL/EXT-10-19329 (Idaho National Lab. (INL), Idaho Falls, ID (United States), 2011).
112. Zhang, P., Xu, J., Shi, L. & Zhang, Z. Nuclear Hydrogen Production Based on High Temperature Gas Cooled Reactor in China. *Strateg. Study Chin. Acad. Eng.* **21**, 20–28 (2019).
113. Ritcher, Z., Davidson, E., Skutnik, S. & Munk, M. *Modeling and Simulation of Xe-100-type Pebble Bed Gas-Cooled Reactor with SCALE*. Technical Report. ORNL/TM-2023/2959 (Oak Ridge National Laboratory (ORNL), Oak Ridge, TN (United States), 2023).
114. Ueta, S. et al. Development of high temperature gas-cooled reactor (HTGR) fuel in Japan. *Prog. Nucl. Energy* **53**, 788–793 (2011).
115. Shibata, T. et al. Present status of JAEA's R&D toward HTGR deployment. *Nucl. Eng. Des.* **398**, 111964 (2022).
116. LeBlanc, D. Molten salt reactors: a new beginning for an old idea. *Nucl. Eng. Des.* **240**, 1644–1656 (2010).
117. Mochizuki, H. Summary of researches on operational characteristics and safety of molten salt fast reactors based on neutronics and thermal-hydraulics coupling analysis. *Nucl. Eng. Des.* **435**, 113941 (2025).
118. Kelleher, B. C., Gagnon, S. F. & Mitchell, I. G. Thermal gradient mass transport corrosion in NaCl-MgCl2 and MgCl2-NaCl-KCl molten salts. *Mater. Today Commun.* **33**, 104358 (2022).
119. Young, G. A., Hacket, M. J. & Sham, T. L. Materials challenges for molten salt reactors. http://inis.iaea.org/Search/search.aspx?orig_q=RN:51012440.
120. Rykhlevskii, A. Chapter 26 - Kairos power pebble bed reactor. In *Molten Salt Reactors and Thorium Energy* 2nd edn (eds Dolan, T. J., Pázsit, I., Rykhlevskii, A. & Yoshioka, R.) Woodhead Publishing Series in Energy, 945–952 (Woodhead Publishing, 2024).
121. Khakim, A., Rhoma, F., Waluyo, A. & Suharyana, S. The neutronic characteristics of thermal molten salt reactor. In *AIP Conference Proceedings* Vol. 2374, 020028 (AIP Publishing LLC, 2021).
122. Dunn, M. Molten salt reactors: current technology status and the challenges for maritime applications. In *Conference Proceedings of INEC* Vol. 2024 (Institute of Marine Engineering, Science and Technology (IMarEST), 2024).
123. Gabriel-Ohanu, E. et al. Optimization of a primary heat exchanger for flibe molten salt nuclear reactor with SCO2 power system. In *Turbo Expo: Power for Land, Sea, and Air* Vol. 85048, V010T30A023 (American Society of Mechanical Engineers, 2021).
124. Locatelli, G., Bingham, C. & Mancini, M. Small modular reactors: a comprehensive overview of their economics and strategic aspects. *Prog. Nucl. Energy* **73**, 75–85 (2014).

125. Ingersoll, D. T. & Carelli, M. D. *Handbook of Small Modular Nuclear Reactors* (Elsevier, 2014). Google-Books-ID: rJIzAwAAQBAJ.
126. Schlegel, J. P. & Bhowmik, P. K. Chapter 14 - Small modular reactors. In *Nuclear Power Reactor Designs* (eds Wang, J., Talabi, S. & Leon, S. B. Y.) 283–308 (Academic Press, 2024).
127. Peakman, A., Hodgson, Z. & Merk, B. Advanced micro-reactor concepts. *Prog. Nucl. Energy* **107**, 61–70 (2018).
128. Testoni, R., Bersano, A. & Segantin, S. Review of nuclear microreactors: status, potentialities and challenges. *Prog. Nucl. Energy* **138**, 103822 (2021).
129. Black, G. et al. Prospects for nuclear microreactors: a review of the technology, economics, and regulatory considerations. *Nucl. Technol.* **209**, S1–S20 (2023).
130. Yan, B. H., Wang, C. & Li, L. G. The technology of micro heat pipe cooled reactor: a review. *Ann. Nucl. Energy* **135**, 106948 (2020).
131. Aldebie, F., Fernandez-Cosials, K. & Hassan, Y. Thermal-mechanical safety analysis of heat pipe micro reactor. *Nucl. Eng. Des.* **420**, 113003 (2024).
132. Duderstadt, J. J. & Hamilton, L. J. *Nuclear Reactor Analysis* (John Wiley and Sons, Inc., 1975).
133. Drzewiecki, T., Schmidt, J., n Wert, C. V. & Clifford, P. *Fuel Qualification For Advanced Reactors, Final (Nureg-2246)* (United States Nuclear Regulatory Commission, 2022).
134. Sridhar, N., Dunn, D. S., Cragnolino, G. & Yang, N. *Nureg/cr-7299: An Integrated Structure and Environment Dependent Corrosion Model for Used Nuclear Fuel Dry Storage Systems*. Technical Report. NUREG/CR-7299 (U.S. Nuclear Regulatory Commission, 2010).
135. Faibish, R. *Accelerated Fuel Qualifcation White Paper*. Technical Report. ML21287A646. Available at https://www.nrc.gov/docs/ML2128/ML21287A646.pdf (General Atomics, 2021).
136. White, A. The materials genome initiative: one year on. *MRS Bull.* **37**, 715–716 (2012).
137. Lemaignan, C. & Motta, A. T. Zirconium alloys in nuclear applications. *Mater. Sci. Technol.* **10**, 1–51 (1994).
138. Woods, C. *Properties of Zircaloy-4 Tubing*. Technical Report. (Bettis Atomic Power Lab.(BAPL), Pittsburgh, PA (United States), 1966).
139. Sabol, G. P. Zirlo™—an alloy development success, j. *ASTM Int* **2**, 3–24 (2005).
140. Mardon, J.-P., Charquet, D. & Senevat, J. Influence of composition and fabrication process on out-of-pile and in-pile properties of m5 alloy. In *Zirconium in the Nuclear Industry: Twelfth International Symposium* (ASTM International, 2000).
141. Tang, C., Stüber, M., Seifert, H. J. & Steinbrück, M. Metallic and ceramic coatings for enhanced accident tolerant fuel cladding. *Compr. Nucl. Mater.* **4**, 490–514 (2020).
142. Ko, J., Kim, J. W., Min, H. W., Kim, Y. & Yoon, Y. S. Review of manufacturing technologies for coated accident tolerant fuel cladding. *J. Nucl. Mater.* **561**, 153562 (2022).
143. Mankins, W. L., Hosier, J. C. & Bassford, T. H. Microstructure and phase stability of INCONEL alloy 617. *Metall. Trans.* **5**, 2579–2590 (1974).
144. McCoy, H. E. & King, J. F. *Mechanical Properties of Inconel 617 and 618*. Technical Report. ORNL/TM-9337 (Oak Ridge National Lab. (ORNL), Oak Ridge, TN (United States) https://doi.org/10.2172/711763. https://www.osti.gov/biblio/711763 (1985).
145. Nickel, H., Schubert, F. & Schuster, H. Evaluation of alloys for advanced high-temperature reactor systems. *Nucl. Eng. Des.* **78**, 251–265 (1984).
146. Ren, W. & Swindeman, R. *A Review of Aging Effects in Alloy 617 for Gen IV Nuclear Reactor Applications* 489–500 (American Society of Mechanical Engineers Digital Collection, 2008).
147. Ren, W. & Swindeman, R. A review on current status of alloys 617 and 230 for Gen IV nuclear reactor internals and heat exchangers 1. *J Pressure Vessel Technol*. **131**, 044002 (2009).
148. Dayton, R., Oxley, J. & Townley, C. Ceramic coated particle nuclear fuels. *J. Nucl. Mater.* **11**, 1–31 (1964).
149. Goeddel, W. Coated-particle fuels in high-temperature reactors: a summary of current applications. *Nucl. Appl.* **3**, 599–614 (1967).
150. Sowder, A. & Marciulescu, C. *Uranium Oxycarbide (UCO) Tristructural Isotropic (triso) Coated Particle Fuel Performance*. Technical Report. Topical Report EPRI-AR-1 (NP), Technical Report (2019).
151. Zhang, F.-Y., Zhu, G.-F., Zou, Y., Yan, R. & Xu, H.-J. Conceptual design and neutronic analysis of a megawatt-level vehicular microreactor based on TRISO fuel particles and S-CO2 direct power generation. *Nucl. Sci. Tech.* **33**, 69 (2022).
152. Skerjanc, W. F. & Youinou, G. J. High uranium loading TRISO particle for microreactor applications. *Nucl. Eng. Des.* **414**, 112628 (2023).
153. DeHart, M. D., Schunert, S. & Labouré, V. M. Nuclear thermal propulsion. In *Nuclear Reactors-Spacecraft Propulsion, Research Reactors, and Reactor Analysis Topics* (IntechOpen, 2022).
154. Kiegiel, K., Herdzik-Koniecko, I., Fuks, L. & Zakrzewska-Kołtuniewicz, G. Management of radioactive waste from HTGR reactors including spent TRISO fuel—state of the art. *Energies* **15**, 1099 (2022).
155. Guittonneau, F., Abdelouas, A. & Grambow, B. Htr fuel waste management: triso separation and acid-graphite intercalation compounds preparation. *J. Nucl. Mater.* **407**, 71–77 (2010).
156. Council, N. R., on Engineering, D., Sciences, P., Board, N. M. A. & on Integrated Computational Materials Engineering, C. *Integrated Computational Materials Engineering: A Transformational Discipline for Improved Competitiveness and National Security* (National Academies Press, 2008).
157. de Pablo, J. J., Jones, B., Kovacs, C. L., Ozolins, V. & Ramirez, A. P. The materials genome initiative, the interplay of experiment, theory and computation. *Curr. Opin. Solid State Mater. Sci.* **18**, 99–117 (2014).
158. de Pablo, J. J. et al. New frontiers for the materials genome initiative. *npj Comput. Mater.* **5**, 1–23 (2019).
159. Attari, V. & Arroyave, R. Machine learning-assisted high-throughput exploration of interface energy space in multi-phase-field model with CALPHAD potential. *Mater. Theory* **6**, 5 (2022).
160. Zhao, Y.-H. Editorial: phase field method and integrated computing materials engineering. *Front. Mater*. **10**, https://doi.org/10.3389/fmats.2023.1145833 (2023).
161. Otis, R. A. & Liu, Z.-K. High-throughput thermodynamic modeling and uncertainty quantification for ICME. *Jom* **69**, 886–892 (2017).
162. Wong, T. T. & Paramsothy, M. Icme after one decade: success and challenges. *JOM* **70**, 1642–1643 (2018).
163. The Minerals, M. M. S. T. *Accelerating the Broad Implementation of Verification & Validation in Computational Models of the Mechanics of Materials and Structures* (TMS, 2020).
164. Olson, G. B. Genomic materials design: the ferrous frontier. *Acta Mater.* **61**, 771–781 (2013).
165. Olson, G. B. & Kuehmann, C. J. Materials genomics: from CALPHAD to flight. *Scr. Mater.* **70**, 25–30 (2014).
166. Taskin, K. High Performance Ferrium Steels for Aerospace Gearing and Bearing Applications. https://doi.org/10.1520/STP162320190055 (2020).
167. Josephson, R. Development of ferrium S53 high-strength, corrosion-resistant steel (2009).
168. Grabowski, J., Sebastian, J., Olson, G., Asphahani, A. & Genellie Jr, R. Integrated computational materials engineering helps successfully develop aerospace alloys. *AMP Tech. Artic.* **171**, 17–19 (2013).
169. Sebastian, J. & Olson, G. Examples of QuesTek Innovations' Application ICME to Materials Design, Development, and Rapid Qualification. In *55th AIAA/ASME/ASCE/AHS/ASC Structures,*

Structural Dynamics, and Materials Conference (American Institute of Aeronautics and Astronautics).
170. Integrated Computational Materials Design: From Genome o Flight. https://doi.org/10.2514/6.2013-1847. https://arc.aiaa.org/doi/10.2514/6.2013-1847.
171. Warren, J. A. The Materials Genome Initiative and the Metals Industry. *Bridge* **54**, 25–30 (2024).
172. Questek. FERRIUM S53: ultrahigh-strength stainless steel. *Alloy Digest* **57**, SS–942 (2008).
173. Questek. FERRIUM M54: martensitic secondary hardening steel. *Alloy Digest* 67, SA–822 (2018).
174. Questek. FERRIUM C64: martensitic secondary hardening steel. *Alloy Digest* **67**, SA–827 (2018).
175. Cao, W. & Kennedy, R. Role of chemistry in 718-type alloys—allvac 718plus alloy development. *Superalloys* **2004**, 91–99 (2004).
176. Kennedy, R. L., Cao, W., Bayha, T. & Jeniski, R. Developments in wrought Nb containing superalloys (718+ 100 f), the mineral. Metals & Materials Society (2003).
177. Xie, X. et al. Structure stability study on a newly developed nickel-base superalloy—allvac® 718plus™. *Superalloys* **718**, 625–706 (2005).
178. Kushan, M. C., Uzgur, S. C., Uzunonat, Y. & Diltemiz, F. Allvac 718 plus™ superalloy for aircraft engine applications. *Recent Adv. Aircr. Technol.* **4**, 75–96 (2012).
179. Zinkle, S. J. & Was, G. S. Materials challenges in nuclear energy. *Acta Mater.* **61**, 735–758 (2013).
180. Tonks, M. R. et al. Mechanistic materials modeling for nuclear fuel performance. *Ann. Nucl. Energy* **105**, 11–24 (2017).
181. Bhowmik, P. K. et al. Integral and Separate effects test facilities to support water cooled small modular reactors: a review. *Prog. Nucl. Energy* **160**, 104697 (2023).
182. Nelson, A. T., Adorno Lopes, D., Capps, N. A. & Petrie, C. M. Role of accelerated burnup irradiation testing in support of accelerated fuel qualification. *Nucl. Technol.* **0**, 1–30 (2025).
183. Choi, H. et al. Accelerated fuel qualification of fast modular reactor fuel in a thermal reactor: modeling and simulation paired with irradiation testing. *Nucl. Technol.* **0**, 1–16 (2025).
184. Zhou, W. et al. Proton irradiation-decelerated intergranular corrosion of Ni-Cr alloys in molten salt. *Nat. Commun.* **11**, 3430 (2020).
185. Was, G. S. Challenges to the use of ion irradiation for emulating reactor irradiation. *J. Mater. Res.* **30**, 1158–1182 (2015).
186. Taller, S., Chen, Y., Song, R., Chen, W.-Y. & Jokisaari, A. An approach to combine neutron and ion irradiation data to accelerate material qualification for nuclear reactors. *J. Nucl. Mater.* **603**, 155385 (2025).
187. Jokisaari, A. M., Taller, S., Chen, Y., Chen, W.-Y. & Song, R. Promoting regulatory acceptance of combined ion and neutron irradiation testing of nuclear reactor materials: Modeling and software considerations. *Prog. Nucl. Energy* **178**, 105518 (2025).
188. Chernatynskiy, A., Phillpot, S. R. & LeSar, R. Uncertainty quantification in multiscale simulation of materials: a prospective. *Annu. Rev. Mater. Res.* **43**, 157–182 (2013).
189. Dienstfrey, A. et al. Uncertainty quantification in materials modeling. *JOM* **66**, 1342–1344 (2014).
190. Honarmandi, P. & Arróyave, R. Uncertainty quantification and propagation in computational materials science and simulation-assisted materials design. *Integr. Mater. Manuf. Innov.* **9**, 103–143 (2020).
191. Matthews, C. et al. Mechanistic multiscale uncertainty propagation in support of accelerated fuel qualification. *Nucl. Technol.* **0**, 1–13 (2025).
192. Notley, M. J. F. & Hastings, I. J. A microstructure-dependent model for fission product gas release and swelling in UO2 fuel. *Nucl. Eng. Des.* **56**, 163–175 (1980).
193. Lewis, B. J., Iglesias, F. C., Cox, D. S. & Gheorghiu, E. A model for fission gas release and fuel oxidation behavior for defected UO2 fuel elements. *Nucl. Technol.* **92**, 353–362 (1990).
194. Lee, B.-H., Koo, Y.-H. & Sohn, D.-S. Modeling of the rim effect on thermal behavior of high-burnup UO2 fuel. *Nucl. Technol.* **127**, 151–159 (1999).
195. Jernkvist, L. O. A continuum model for cracked UO2 fuel. *Nucl. Eng. Des.* **176**, 273–284 (1997).
196. Loewen, E. P., Wilson, R. D., Hohorst, J. K. & Kumar, A. S. Preliminary FRAPCON-3Th Steady-state fuel analysis of ThO2 and UO2 fuel mixtures. *Nucl. Technol.* **136**, 261–277 (2001).
197. Lee, B.-H., Koo, Y.-H., Oh, J.-Y., Cheon, J.-S. & Sohn, D.-S. Improvement of fuel performance code COSMOS with recent in-pile data for MOX and UO2 fuels. *Nucl. Technol.* **157**, 53–64 (2007).
198. Rossiter, G. Development of the enigma fuel performance code for whole core analysis and dry storage assessments. *Nucl. Eng. Technol.* **43**, 489–498 (2011).
199. Demarco, G. L. & Marino, A. C. 3D finite elements modelling for design and performance analysis of UO2 pellets. *Sci. Technol. Nucl. Install.* **2011**, 843491 (2011).
200. Rashid, J. Y. R., Yagnik, S. K. & Montgomery, R. O. Light water reactor fuel performance modeling and multi-dimensional simulation. *JOM* **63**, 81–88 (2011).
201. Walker, J. & Catlow, C. Structural and dynamic properties of UO2 at high temperatures. *J. Phys. C: Solid State Phys.* **14**, L979 (1981).
202. Yamada, K., Kurosaki, K., Uno, M. & Yamanaka, S. Evaluation of thermal properties of uranium dioxide by molecular dynamics. *J. Alloy. Compd.* **307**, 10–16 (2000).
203. Morelon, N.-D., Ghaleb, D., Delaye, J.-M. & Van Brutzel, L. A new empirical potential for simulating the formation of defects and their mobility in uranium dioxide. *Philos. Mag.* **83**, 1533–1555 (2003).
204. Basak, C. B., Sengupta, A. K. & Kamath, H. S. Classical molecular dynamics simulation of UO2 to predict thermophysical properties. *J. Alloy. Compd.* **360**, 210–216 (2003).
205. Arima, T., Yamasaki, S., Inagaki, Y. & Idemitsu, K. Evaluation of thermal properties of UO2 and PuO2 by equilibrium molecular dynamics simulations from 300 to 2000 K. *J. Alloy. Compd.* **400**, 43–50 (2005).
206. Meis, C. & Chartier, A. Calculation of the threshold displacement energies in UO2 using ionic potentials. *J. Nucl. Mater.* **341**, 25–30 (2005).
207. Skomurski, F. N., Ewing, R. C., Rohl, A. L., Gale, J. D. & Becker, U. Quantum mechanical vs. empirical potential modeling of uranium dioxide (UO2) surfaces: (111), (110), and (100). *Am. Mineral.* **91**, 1761–1772 (2006).
208. Yakub, E., Ronchi, C. & Staicu, D. Molecular dynamics simulation of premelting and melting phase transitions in stoichiometric uranium dioxide. *J. Chem. Phys.* **127**, 094508 (2007).
209. Goel, P., Choudhury, N. & Chaplot, S. L. Atomistic modeling of the vibrational and thermodynamic properties of uranium dioxide, UO2. *J. Nucl. Mater.* **377**, 438–443 (2008).
210. Govers, K., Lemehov, S., Hou, M. & Verwerft, M. Comparison of interatomic potentials for UO2. Part I: Static calculations. *J. Nucl. Mater.* **366**, 161–177 (2007).
211. Govers, K., Lemehov, S., Hou, M. & Verwerft, M. Comparison of interatomic potentials for UO2. *J. Nucl. Mater.* **376**, 66–77 (2008).
212. Watanabe, T. et al. Thermal transport properties of uranium dioxide by molecular dynamics simulations. *J. Nucl. Mater.* **375**, 388–396 (2008).
213. Williamson, R. L. et al. Multidimensional multiphysics simulation of nuclear fuel behavior. *J. Nucl. Mater.* **423**, 149–163 (2012).
214. Williamson, R. L. et al. BISON: a flexible code for advanced simulation of the performance of multiple nuclear fuel forms. *Nucl. Technol.* **207**, 954–980 (2021).

215. Tonks, M. R., Zhang, Y., Bai, X. & Millett, P. C. Demonstrating the temperature gradient impact on grain growth in UO2 using the phase field method. *Mater. Res. Lett.* **2**, 23–28 (2014).
216. Tonks, M. R., Zhang, Y., Butterfield, A. & Bai, X.-M. Development of a grain boundary pinning model that considers particle size distribution using the phase field method. *Model. Simul. Mater. Sci. Eng.* **23**, 045009 (2015).
217. Tonks, M. R., Simon, P.-C. A. & Hirschhorn, J. Mechanistic grain growth model for fresh and irradiated UO2 nuclear fuel. *J. Nucl. Mater.* **543**, 152576 (2021).
218. Andersson, D. A., Uberuaga, B. P., Nerikar, P. V., Unal, C. & Stanek, C. R. U and Xe transport in UO2: Density functional theory calculations. *Phys. Rev. B* **84**, 054105 (2011).
219. Millett, P. C., Zhang, Y., Tonks, M. R. & Biner, S. B. Consideration of grain size distribution in the diffusion of fission gas to grain boundaries. *J. Nucl. Mater.* **440**, 435–439 (2013).
220. Andersson, D. A. et al. Atomistic modeling of intrinsic and radiation-enhanced fission gas (Xe) diffusion in : Implications for nuclear fuel performance modeling. *J. Nucl. Mater.* **451**, 225–242 (2014).
221. Millett, P. C., Tonks, M. R. & Biner, S. B. Grain boundary percolation modeling of fission gas release in oxide fuels. *J. Nucl. Mater.* **424**, 176–182 (2012).
222. Millett, P. C. et al. Phase-field simulation of intergranular bubble growth and percolation in bicrystals. *J. Nucl. Mater.* **425**, 130–135 (2012).
223. Aagesen, L. K., Schwen, D., Tonks, M. R. & Zhang, Y. Phase-field modeling of fission gas bubble growth on grain boundaries and triple junctions in UO2 nuclear fuel. *Comput. Mater. Sci.* **161**, 35–45 (2019).
224. Phillpot, S. R., El-Azab, A., Chernatynskiy, A. & Tulenko, J. S. Thermal conductivity of UO2 fuel: Predicting fuel performance from simulation. *JOM* **63**, 73–79 (2011).
225. Chockalingam, K., Millett, P. C. & Tonks, M. R. Effects of intergranular gas bubbles on thermal conductivity. *J. Nucl. Mater.* **430**, 166–170 (2012).
226. Tonks, M. R. et al. Multiscale development of a fission gas thermal conductivity model: Coupling atomic, meso and continuum level simulations. *J. Nucl. Mater.* **440**, 193–200 (2013).
227. Tonks, M. R. et al. Development of a multiscale thermal conductivity model for fission gas in UO2. *J. Nucl. Mater.* **469**, 89–98 (2016).
228. Chakraborty, P., Tonks, M. R. & Pastore, G. Modeling the influence of bubble pressure on grain boundary separation and fission gas release. *J. Nucl. Mater.* **452**, 95–101 (2014).
229. Chakraborty, P., Zhang, Y. & Tonks, M. R. Multi-scale modeling of microstructure dependent intergranular brittle fracture using a quantitative phase-field based method. *Comput. Mater. Sci.* **113**, 38–52 (2016).
230. Jiang, W., Hu, T., Aagesen, L. K. & Zhang, Y. Three-dimensional phase-field modeling of porosity dependent intergranular fracture in UO2. *Comput. Mater. Sci.* **171**, 109269 (2020).
231. Neilson, W. D., Galvin, C. O. T., Dillon, S. J., Cooper, M. W. D. & Andersson, D. A. Irradiation-induced creep in UO_2: The role of grain boundaries. *Phys. Rev. Mater.* **8**, 103602 (2024).
232. Galvin, C. O. T., Andersson, D. A., Sweet, R. T., Capolungo, L. & Cooper, M. W. D. Diffusional creep model in UO2 informed by lower-length scale simulations. *J. Nucl. Mater.* **607**, 155659 (2025).
233. Xiao, H., Long, C. & Chen, H. Model for evolution of grain size in the rim region of high burnup UO2 fuel. *J. Nucl. Mater.* **471**, 74–79 (2016).
234. Bai, X.-M., Tonks, M. R., Zhang, Y. & Hales, J. D. Multiscale modeling of thermal conductivity of high burnup structures in UO2 fuels. *J. Nucl. Mater.* **470**, 208–215 (2016).
235. Veshchunov, M. & Tarasov, V. Modelling of pore coarsening in the high burn-up structure of uo2 fuel. *J. Nucl. Mater.* **488**, 191–195 (2017).
236. Abdoelatef, M. G. et al. Mesoscale modeling of high burn-up structure formation and evolution in UO2. *JOM* **71**, 4817–4828 (2019).
237. Barani, T. et al. Modeling high burnup structure in oxide fuels for application to fuel performance codes. part I: High burnup structure formation. *J. Nucl. Mater.* **539**, 152296 (2020).
238. Brinkley, W. C., Capps, N. & Wirth, B. An initial microstructurally informed model of high burnup structure formation in UO2 Fuel. *Nucl. Sci. Eng.* **0**, 1–16 (2025).
239. Biswas, S. & Aagesen, L. K. Mesoscale modeling of restructuring in high burnup UO_2 fuel. *Comput. Mater. Sci.* **258**, 114052 (2025).
240. Capps, N., Schappel, D. & Nelson, A. Initial development of an RIA envelope for dispersed nuclear fuel. *Ann. Nucl. Energy* **148**, 107719 (2020).
241. Khvostov, G. Analytical criteria for fuel fragmentation and burst FGR during a LOCA. *Nucl. Eng. Technol.* **52**, 2402–2409 (2020).
242. Capps, N., Sweet, R., Harp, J. & Petrie, C. M. High-burnup fuel stress analysis prior to and during a local transient. *J. Nucl. Mater.* **556**, 153194 (2021).
243. Jiang, W., Hu, T., Aagesen, L. K., Biswas, S. & Gamble, K. A. A phase-field model of quasi-brittle fracture for pressurized cracks: application to UO_2 high-burnup microstructure fragmentation. *Theor. Appl. Fract. Mech.* **119**, 103348 (2022).
244. Zhang, S., Jiang, W., Gamble, K. A. & Tonks, M. R. Comparing the impact of thermal stresses and bubble pressure on intergranular fracture in UO2 using 2D phase field fracture simulations. *J. Nucl. Mater.* **574**, 154158 (2023).
245. Greenquist, I., Wysocki, A., Hirschhorn, J. & Capps, N. Multiphysics analysis of fuel fragmentation, relocation, and dispersal susceptibility-Part 1: overview and code coupling strategies. *Ann. Nucl. Energy* **191**, 109913 (2023).
246. Hirschhorn, J., Greenquist, I., Wysocki, A. & Capps, N. Multiphysics analysis of fuel fragmentation, relocation, and dispersal susceptibility–part 2: High-burnup steady-state operating and fuel performance conditions. *Ann. Nucl. Energy* **192**, 109952 (2023).
247. Gencturk, M. et al. Thermo-mechanical phase-field modeling of fracture in high-burnup UO2 fuels under transient conditions. *Materials* **18**, https://doi.org/10.3390/ma18051162 (2025).
248. Pastore, G. et al. Modelling of transient fission gas behaviour in oxide fuel and application to the BISON Code. In *Enlarged Halden Programme Group Meeting, Røros, Norway* (2014).
249. Capps, N. et al. Empirical and mechanistic transient fission gas release model for high-burnup LOCA conditions. *J. Nucl. Mater.* **584**, 154557 (2023).
250. Lieou, C. K. C., Capps, N. A., Cooper, M. W. D., Simon, P.-C. A. & Wirth, B. D. An integrated statistical-thermodynamic model for fission gas release and swelling in nuclear fuels. *J. Nucl. Mater.* **589**, 154869 (2024).
251. ARBORELIUS, J. et al. Advanced Doped UO2 Pellets in LWR Applications. *J. Nucl. Sci. Technol.* **43**, 967–976 (2006).
252. Cooper, M. W. D., Stanek, C. R. & Andersson, D. A. The role of dopant charge state on defect chemistry and grain growth of doped UO2. *Acta Mater.* **150**, 403–413 (2018).
253. Owen, M. W. et al. Diffusion in undoped and Cr-doped amorphous UO2. *J. Nucl. Mater.* **576**, 154270 (2023).
254. Kocevski, V., Cooper, M. W. D. & Andersson, D. A. Modeling of fission gas diffusion and release for doped. *J. Nucl. Mater.* **584**, 154575 (2023).
255. Greenquist, I., Tonks, M., Cooper, M., Andersson, D. & Zhang, Y. Grand potential sintering simulations of doped UO2 accident-tolerant fuel concepts. *J. Nucl. Mater.* **532**, 152052 (2020).
256. Gamble, K. A., Pastore, G. & Cooper, M. W. D. *BISON Development and Validation for Priority LWR-ATF Concepts*. Technical Report. INL/EXT-20-59969-Rev000 (Idaho National Lab. (INL), Idaho Falls,

ID (United States) https://doi.org/10.2172/1717844. https://www.osti.gov/biblio/1717844 (2020).
257. Cooper, M. W. D., Andersson, A. D. R. & Stanek, C. R. *Mn-Doped Oxide Nuclear Fuel*. Technical Report. 10,847,271 (Los Alamos National Laboratory (LANL), Los Alamos, NM (United States) https://www.osti.gov/biblio/1771664 (2020).
258. Badry, F., Brito, R., Abdoelatef, M. G., McDeavitt, S. & Ahmed, K. An experimentally validated mesoscale model of thermal conductivity of a UO2 and BeO composite nuclear fuel. *JOM* **71**, 4829–4838 (2019).
259. Hilty, F. W. & Tonks, M. R. Development and application of a microstructure dependent thermal resistor model for UO2 reactor fuel with high thermal conductivity additives. *J. Nucl. Mater.* **540**, 152334 (2020).
260. Sweidan, F., Costa, D. R., Liu, H. & Olsson, P. Temperature-dependent thermal conductivity and fuel performance of UN-UO2 and UN-X-UO2 (X=Mo, W) composite nuclear fuels by finite element modeling. *J. Mater.* **10**, 937–946 (2024).
261. Hilty, F. W., Kim, D.-U. & Tonks, M. R. Impact of fission gas bubbles on thermal conductivity of UO2 fuels with high thermal conductivity additives. *J. Nucl. Mater.* **546**, 152779 (2021).
262. Cheniour, A. et al. Development of a grain growth model for U3Si2 using experimental data, phase field simulation and molecular dynamics. *J. Nucl. Mater.* **532**, 152069 (2020).
263. Aagesen, L. K. et al. Phase-field simulations of intergranular fission gas bubble behavior in U3Si2 nuclear fuel. *J. Nucl. Mater.* **541**, 152415 (2020).
264. Gamble, K. A. et al. Improvement of the BISON U3Si2 modeling capabilities based on multiscale developments to modeling fission gas behavior. *J. Nucl. Mater.* **555**, 153097 (2021).
265. Andersson, D. A., Stanek, C. R., Matthews, C. & Uberuaga, B. P. The past, present, and future of nuclear fuel. *MRS Bull.* **48**, 1154–1162 (2023).
266. Ducher, R., Dubourg, R., Barrachin, M. & Pasturel, A. First-principles study of defect behavior in irradiated uranium monocarbide. *Phys. Rev. B* **83**, 104107 (2011).
267. Freyss, M. First-principles study of uranium carbide: accommodation of point defects and of helium, xenon, and oxygen impurities. *Phys. Rev. B* **81**, 014101 (2010).
268. Basak, C. B. Classical molecular dynamics simulation of uranium monocarbide (UC). *Comput. Mater. Sci.* **40**, 562–568 (2007).
269. Chartier, A. & Van Brutzel, L. Modeling of point defects and rare gas incorporation in uranium mono-carbide. *Nucl. Instrum. Methods Phys. Res. Sect. B Beam Interact. Mater.* **255**, 146–150 (2007).
270. Mankad, V. H. & Jha, P. K. Thermodynamic properties of nuclear material uranium carbide using density functional theory. *J. Therm. Anal. Calorim.* **124**, 11–20 (2016).
271. Mei, Z.-G., Ye, B., Yacout, A. M., Beeler, B. & Gao, Y. First-principles study of the surface properties of uranium carbides. *J. Nucl. Mater.* **542**, 152257 (2020).
272. Kocevski, V., Cooper, M. W. D., Claisse, A. J. & Andersson, D. A. Development and application of a uranium mononitride (UN) potential: thermomechanical properties and Xe diffusion. *J. Nucl. Mater.* **562**, 153553 (2022).
273. AbdulHameed, M., Beeler, B., Galvin, C. O. T. & Cooper, M. W. D. Assessment of uranium nitride interatomic potentials. *J. Nucl. Mater.* **600**, 155247 (2024).
274. Kocevski, V., Rehn, D. A., Cooper, M. W. D. & Andersson, D. A. First-principles investigation of uranium mononitride (UN): Effect of magnetic ordering, spin-orbit interactions and exchange correlation functional. *J. Nucl. Mater.* **559**, 153401 (2022).
275. Cooper, M. W. D. et al. Simulations of self- and Xe diffusivity in uranium mononitride including chemistry and irradiation effects. *J. Nucl. Mater.* **587**, 154685 (2023).
276. Schneider, A. et al. Radiation induced athermal diffusivity in uranium mononitride. *J. Nucl. Mater.* **601**, 155313 (2024).
277. Kocevski, V. et al. Finite temperature properties of uranium mononitride. *J. Nucl. Mater.* **576**, 154241 (2023).
278. Kocevski, V. et al. CALPHAD modeling of uranium nitride (UN) fabrication routes enabled by first-principles calculations. *Calphad* **79**, 102463 (2022).
279. Rizk, J. T. et al. Mechanistic nuclear fuel performance modeling of uranium nitride. *J. Nucl. Mater.* **606**, 155604 (2025).
280. Billone, M. C., Liu, Y. Y., Gruber, E. E., Hughes, T. H. & Kramer, J. M. Status of Fuel Element Modeling Codes for Metallic Fuels. In *Proc. American Nuclear Society International Conference on Reliable Fuels for Liquid Metal Reactors* (American Nuclear Society (ANS), Tucson, Arizona, 1968).
281. Kobayashi, T. et al. Development of the SESAME metallic fuel performance code. *Nucl. Technol.* **89**, 183–193 (1990).
282. Hwang, W., Nam, C., Byun, T. S. & Kim, Y. C. MACSIS: a metallic fuel performance analysis code for simulating in-reactor behavior under steady-state conditions. *Nucl. Technol.* **123**, 130–141 (1998).
283. Ogata, T. & Yokoo, T. Development and Validation of ALFUS: an irradiation behavior analysis code for metallic fast reactor fuels. *Nucl. Technol.* **128**, 113–123 (1999).
284. Galloway, J., Unal, C., Carlson, N., Porter, D. & Hayes, S. Modeling constituent redistribution in U-Pu-Zr metallic fuel using the advanced fuel performance code BISON. *Nucl. Eng. Des.* **286**, 1–17 (2015).
285. Hou, Y. et al. U-50Zr helical cruciform fuel performance analysis based on MOOSE framework. *Ann. Nucl. Energy* **204**, 110529 (2024).
286. Chen, X., Xie, Z., Mao, X. & Ding, S. Modeling of zirconium atom redistribution and phase transformation coupling behaviors in U-10Zr-based helical cruciform fuel rods under irradiation. *Metals* **14**, 745 (2024).
287. Beeler, B. et al. First principles calculations for defects in U. *J. Phys. Condens. Matter* **22**, 505703 (2010).
288. Huang, G.-Y. & Wirth, B. D. First-principles study of diffusion of interstitial and vacancy in α U-Zr. *J. Phys. Condens. Matter* **23**, 205402 (2011).
289. Beeler, B., Deo, C., Baskes, M. & Okuniewski, M. Atomistic properties of γ uranium. *J. Phys. Condens. Matter* **24**, 075401 (2012).
290. Beeler, B., Deo, C., Baskes, M. & Okuniewski, M. Atomistic Investigations of Intrinsic and Extrinsic Point Defects in bcc Uranium. In *Atomistic Investigations of Intrinsic and Extrinsic Point Defects in bcc Uranium* (2013).
291. Xiong, W., Xie, W., Shen, C. & Morgan, D. Thermodynamic modeling of the U-Zr system—a revisit. *J. Nucl. Mater.* **443**, 331–341 (2013).
292. Moore, A. P., Beeler, B., Deo, C., Baskes, M. I. & Okuniewski, M. A. Atomistic modeling of high temperature uranium-zirconium alloy structure and thermodynamics. *J. Nucl. Mater.* **467**, 802–819 (2015).
293. Moore, A. P., Deo, C., Baskes, M. I. & Okuniewski, M. A. Atomistic mechanisms of morphological evolution and segregation in U-Zr alloys. *Acta Mater.* **115**, 178–188 (2016).
294. Hirschhorn, J., Tonks, M., Aitkaliyeva, A. & Adkins, C. Development and verification of a phase-field model for the equilibrium thermodynamics of U-Pu-Zr. *Ann. Nucl. Energy* **124**, 490–502 (2019).
295. Hirschhorn, J., Aitkaliyeva, A., Adkins, C. & Tonks, M. The microstructure and thermodynamic behavior of as-cast U-24Pu-15Zr: unexpected results and recommendations for U-Pu-Zr fuel research methodology. *J. Nucl. Mater.* **518**, 80–94 (2019).
296. Hirschhorn, J., Tonks, M., Aitkaliyeva, A. & Adkins, C. Reexamination of a U-Zr diffusion couple experiment using quantitative phase-field modeling and sensitivity analysis. *J. Nucl. Mater.* **529**, 151929 (2020).

297. Hirschhorn, J., Tonks, M. R., Aitkaliyeva, A. & Adkins, C. A study of constituent redistribution in U-Zr fuels using quantitative phase-field modeling and sensitivity analysis. *J. Nucl. Mater.* **523**, 143–156 (2019).
298. Hirschhorn, J., Tonks, M. & Matthews, C. A CALPHAD-informed approach to modeling constituent redistribution in Zr-based metallic fuels using BISON. *J. Nucl. Mater*. **544**, 152657 (2020).
299. Jung, W., Kim, J.-S. & Chang, K. Investigating constituent redistribution in U-Zr metallic fuels: A phase-field approach incorporating porosity and sodium infiltration. *Ann. Nucl. Energy* **224**, 111679 (2025).
300. Zhou, S. et al. Combined ab initio and empirical model of the thermal conductivity of uranium, uranium-zirconium, and uranium-molybdenum. *Phys. Rev. Mater.* **2**, 083401 (2018).
301. Ortega, L. H., Blamer, B., Stern, K. M., Vollmer, J. & McDeavitt, S. M. Thermal conductivity of uranium metal and uranium-zirconium alloys fabricated via powder metallurgy. *J. Nucl. Mater.* **531**, 151982 (2020).
302. Zhou, S., Zhang, Y. & Morgan, D. An ab-initio based semi-empirical thermal conductivity model for multiphase uranium-zirconium alloys. *J. Nucl. Mater.* **553**, 153044 (2021).
303. Chen, W. & Bai, X.-M. Mesoscale modeling of microstructure-dependent thermal conductivity in U-Zr fuels. *J. Nucl. Mater.* **562**, 153593 (2022).
304. Huang, G.-Y. & Wirth, B. D. First-principles study of bubble nucleation and growth behaviors in $\char"03B1$ U-Zr. *J. Phys. Condens. Matter* **24**, 415404 (2012).
305. Smirnova, D. E. et al. A ternary EAM interatomic potential for U-Mo alloys with xenon. *Model. Simul. Mater. Sci. Eng.* **21**, 035011 (2013).
306. Smirnova, D. E., Kuksin, A. Y., Starikov, S. V. & Stegailov, V. V. Atomistic modeling of the self-diffusion in γ-U and γ-U-Mo. *Phys. Met. Metallogr.* **116**, 445–455 (2015).
307. Smirnova, D. E., Kuksin, A. Y. & Starikov, S. V. Investigation of point defects diffusion in bcc uranium and U-Mo alloys. *J. Nucl. Mater.* **458**, 304–311 (2015).
308. Kolotova, L. N., Starikov, S. V. & Ozrin, V. D. Atomistic simulation of the fission-fragment-induced formation of defects in a uranium-molybdenum alloy. *J. Exp. Theor. Phys.* **129**, 59–65 (2019).
309. Xu, Z. et al. Modeling the homogenization kinetics of as-cast U-10wt % Mo alloys. *J. Nucl. Mater.* **471**, 154–164 (2016).
310. Wang, X. et al. Modeling early-stage processes of U-10 Wt.%Mo alloy using integrated computational materials engineering concepts. *JOM* **69**, 2532–2537 (2017).
311. Chakraborty, S., Choudhuri, G., Somayajulu, P. S., Agarwal, R. & Khan, K. B. Microstructure characterization and phase field analysis of dendritic crystal growth of γ-U and BCC-Mo dendrite in U-33 at.% Mo fast reactor fuel. *J. Mater. Res.* **33**, 225–238 (2018).
312. Lu, Y. et al. A phase-field study of spinodal decomposition impeded by irradiation in U-Mo and U-Mo-Zr alloys. *Materials* **16**, 7546 (2023).
313. Liang, L., Mei, Z.-G., Soo Kim, Y., Anitescu, M. & Yacout, A. M. Three-dimensional phase-field simulations of intragranular gas bubble evolution in irradiated U-Mo fuel. *Comput. Mater. Sci.* **145**, 86–95 (2018).
314. Liang, L., Kim, Y. S., Mei, Z.-G., Aagesen, L. K. & Yacout, A. M. Fission gas bubbles and recrystallization-induced degradation of the effective thermal conductivity in U-7Mo fuels. *J. Nucl. Mater.* **511**, 438–445 (2018).
315. Hu, S., Setyawan, W., Beeler, B. W., Gan, J. & Burkes, D. E. Defect cluster and nonequilibrium gas bubble associated growth in irradiated UMo fuels—a cluster dynamics and phase field model. *J. Nucl. Mater.* **542**, 152441 (2020).
316. Lan, X., Jiang, Y., La, Y. & Liu, W. Calculation of the effective thermal conductivity of porous polycrystalline U-10Mo alloy based on phase-field simulation. *Nucl. Eng. Des.* **413**, 112552 (2023).
317. Jiang, Y., Gao, S., La, Y. & Liu, W. Formation of gas bubble superlattice in U-Mo alloys: A phase-field study. *Nucl. Eng. Des.* **435**, 113912 (2025).
318. Beeler, B., Hu, S., Zhang, Y. & Gao, Y. A improved equation of state for Xe gas bubbles in γ U-Mo fuels. *J. Nucl. Mater.* **530**, 151961 (2020).
319. Beeler, B., Casagranda, A., Aagesen, L., Zhang, Y. & Novascone, S. Atomistic calculations of the surface energy as a function of composition and temperature in γ U-Zr to inform fuel performance modeling. *J. Nucl. Mater.* **540**, 152271 (2020).
320. Beeler, B., Cooper, M. W. D., Mei, Z.-G., Schwen, D. & Zhang, Y. Radiation driven diffusion in γU-Mo. *J. Nucl. Mater.* **543**, 152568 (2021).
321. Iasir, A. R. M. & Hammond, K. D. Xenon mobility in γ-uranium and uranium-molybdenum alloys. *J. Appl. Phys.* **131**, 025105 (2022).
322. Potter, P. E. Over forty years of 'Thermodynamics of Nuclear Materials'. *J. Nucl. Mater.* **389**, 29–44 (2009).
323. Besmann, T. M., McMurray, J. W. & Simunovic, S. Application of thermochemical modeling to assessment/evaluation of nuclear fuel behavior. *Calphad* **55**, 47–51 (2016).
324. Matthews, C., Perriot, R., Cooper, M. W. D., Stanek, C. R. & Andersson, D. A. Cluster dynamics simulation of uranium self-diffusion during irradiation in UO2. *J. Nucl. Mater.* **527**, 151787 (2019).
325. Matthews, C., Perriot, R., Cooper, M. W. D., Stanek, C. R. & Andersson, D. A. Cluster dynamics simulation of xenon diffusion during irradiation in UO2. *J. Nucl. Mater.* **540**, 152326 (2020).
326. Liu, X. Y. et al. Atomistic and cluster dynamics modeling of fission gas (Xe) diffusivity in TRISO fuel kernels. *J. Nucl. Mater.* **561**, 153539 (2022).
327. McMurray, J. W. & Besmann, T. M. Thermodynamic Modeling of Nuclear Fuel Materials. In *Handbook of Materials Modeling* 1–29 (Springer, 2018).
328. Corcoran, E. C., Kaye, M. H. & Piro, M. H. A. An overview of thermochemical modelling of CANDU fuel and applications to the nuclear industry. *Calphad* **55**, 52–62 (2016).
329. Piro, M. H. A., Besmann, T. M., Simunovic, S., Lewis, B. J. & Thompson, W. T. Numerical verification of equilibrium thermodynamic computations in nuclear fuel performance codes. *J. Nucl. Mater.* **414**, 399–407 (2011).
330. Piro, M. H. A. Thermodynamically informed nuclear fuel codes—a review and perspectives. *Thermo* **1**, 262–285 (2021).
331. Guéneau, C. et al. TAF-ID: an international thermodynamic database for nuclear fuels applications. *Calphad* **72**, 102212 (2021).
332. Wooding, S. J. & Bacon, D. J. A molecular dynamics study of displacement cascades in α-zirconium. *Philos. Mag. A* **76**, 1033–1051 (1997).
333. Wooding, S. J., Howe, L. M., Gao, F., Calder, A. F. & Bacon, D. J. A molecular dynamics study of high-energy displacement cascades in α-zirconium. *J. Nucl. Mater.* **254**, 191–204 (1998).
334. Rossi, M. L. & Taylor, C. D. Atomistic simulations of formation of elementary Zr-I systems. *Open J. Phys. Chem.* **1**, 104–108 (2011).
335. Rossi, M. L., Taylor, C. D. & van Duin, A. C. Reduced yield stress for zirconium exposed to iodine: reactive force field simulation. *Adv. Model. Simul. Eng. Sci.* **1**, 19 (2014).
336. Rossi, M. L. & Taylor, C. D. First-principles insights into the nature of zirconium-iodine interactions and the initiation of iodine-induced stress-corrosion cracking. *J. Nucl. Mater.* **458**, 1–10 (2015).
337. Taylor, C. D. & Rossi, M. L. Multiphysics modeling of the role of iodine in environmentally assisted cracking of zirconium via pellet-clad interaction. *Corrosion* **72**, 978–988 (2016).
338. Christensen, M. et al. Diffusion of point defects, nucleation of dislocation loops, and effect of hydrogen in hcp-Zr: ab initio and classical simulations. *J. Nucl. Mater.* **460**, 82–96 (2015).

339. Arjhangmehr, A. & Feghhi, S.aH. Irradiation deformation near different atomic grain boundaries in α-Zr: an investigation of thermodynamics and kinetics of point defects. *Sci. Rep.* **6**, 23333 (2016).
340. Sahi, Q. -u-a & Kim, Y.-S. Molecular dynamics simulations of the coupled effects of strain and temperature on displacement cascades in α-zirconium. *Nucl. Eng. Technol.* **50**, 907–914 (2018).
341. Christiaen, B., Domain, C., Thuinet, L., Ambard, A. & Legris, A. A new scenario for <c> vacancy loop formation in zirconium based on atomic-scale modeling. *Acta Mater.* **179**, 93–106 (2019).
342. Maxwell, C., Pencer, J. & Torres, E. Atomistic simulation study of clustering and evolution of irradiation-induced defects in zirconium. *J. Nucl. Mater.* **531**, 151979 (2020).
343. Sakaël, C., Domain, C., Ambard, A., Thuinet, L. & Legris, A. Modelling of zirconium growth under irradiation and annealing conditions. *Int. J. Plast.* **168**, 103699 (2023).
344. Ghorbani, A., Luo, Y., Saidi, P. & Béland, L. K. Anisotropic diffusion of radiation-induced self-interstitial clusters in HCP zirconium: a molecular dynamics and rate-theory assessment. *Scr. Mater.* **238**, 115755 (2024).
345. Jia, X., Bao, Y., Cao, S., Su, Y. & Qian, P. Temperature effects on radiation damage in HCP-zirconium: a molecular dynamics study using a fine-tuned machine-learned potential. *J. Nucl. Mater.* **616**, 156025 (2025).
346. Bai, X.-M., Zhang, Y. & R. Tonks, M. Strain effects on oxygen transport in tetragonal zirconium dioxide. *Phys. Chem. Chem. Phys.* **15**, 19438–19449 (2013).
347. Siripurapu, R. K., Szpunar, B. & Szpunar, J. A. Molecular dynamics study of hydrogen in α-zirconium. *Int. J. Nucl. Energy* **2014**, 912369 (2014).
348. Glazoff, M. V., Tokuhiro, A., Rashkeev, S. N. & Sabharwall, P. Oxidation and hydrogen uptake in zirconium, Zircaloy-2 and Zircaloy-4: computational thermodynamics and ab initio calculations. *J. Nucl. Mater.* **444**, 65–75 (2014).
349. Chakraborty, P., Moitra, A. & Saha-Dasgupta, T. Effect of hydrogen on degradation mechanism of zirconium: a molecular dynamics study. *J. Nucl. Mater.* **466**, 172–178 (2015).
350. Zhang, Y. et al. Homogeneous hydride formation path in α-Zr: Molecular dynamics simulations with the charge-optimized many-body potential. *Acta Mater.* **111**, 357–365 (2016).
351. Wimmer, E. et al. Hydrogen in zirconium: atomistic simulations of diffusion and interaction with defects using a new embedded atom method potential. *J. Nucl. Mater.* **532**, 152055 (2020).
352. Brimbal, D., Chaari, N., Barberis, P. & Bourlier, F. Zirconium-applied anisotropic cluster dynamics for irradiation-induced defect modeling in presence of hydrogen. In *Zirconium in the Nuclear Industry: 19th International Symposium* Vol. STP1622-EB, (eds Motta, A. T. & Yagnik, S. K.) (ASTM International, 2021).
353. Yu, F., Xiang, X., Zu, X. & Hu, S. Hydrogen diffusion in zirconium hydrides from on-the-fly machine learning molecular dynamics. *Int. J. Hydrog. Energy* **56**, 1057–1066 (2024).
354. Mamivand, M., Asle Zaeem, M., El Kadiri, H. & Chen, L.-Q. Phase field modeling of the tetragonal-to-monoclinic phase transformation in zirconia. *Acta Mater.* **61**, 5223–5235 (2013).
355. Asle Zaeem, M. & El Kadiri, H. An elastic phase field model for thermal oxidation of metals: Application to zirconia. *Comput. Mater. Sci.* **89**, 122–129 (2014).
356. Dykhuis, A. F. & Short, M. P. Phase field modeling of irradiation-enhanced corrosion of Zircaloy-4 in PWRs. *Corros. Sci.* **146**, 179–191 (2019).
357. Lin, C., Ruan, H. & Shi, S.-Q. Mechanical-chemical coupling phase-field modeling for inhomogeneous oxidation of zirconium induced by stress-oxidation interaction. *npj Mater. Degrad.* **4**, 22 (2020).
358. Xin, T., Kharchenko, D. O., Kharchenko, V. O. & Lu, W. Phase field modeling of sub-parabolic oxidation kinetics and in-plane stress in zircaloy under neutron/proton irradiation. *Phys. Scr.* **100**, 035941 (2025).
359. Ma, X. Q., Shi, S. Q., Woo, C. H. & Chen, L. Q. Simulation of γ-hydride precipitation in bi-crystalline zirconium under uniformly applied load. *Mater. Sci. Eng.: A* **334**, 6–10 (2002).
360. Ma, X. Q., Shi, S. Q., Woo, C. H. & Chen, L. Q. Effect of applied load on nucleation and growth of γ-hydrides in zirconium. *Comput. Mater. Sci.* **23**, 283–290 (2002).
361. Ma, X. Q., Shi, S. Q., Woo, C. H. & Chen, L. Q. Phase-field simulation of hydride precipitation in bi-crystalline zirconium. *Scr. Mater.* **47**, 237–241 (2002).
362. Guo, X., Shi, S.-Q., Zhang, Q. & Ma, X. An elastoplastic phase-field model for the evolution of hydride precipitation in zirconium. Part I: smooth specimen. *J. Nucl. Mater.* **378**, 110–119 (2008).
363. Guo, X. H., Shi, S. Q., Zhang, Q. M. & Ma, X. Q. An elastoplastic phase-field model for the evolution of hydride precipitation in zirconium. Part II: specimen with flaws. *J. Nucl. Mater.* **378**, 120–125 (2008).
364. Zhao, Z. et al. Characterization of Zirconium Hydrides and Phase Field Approach to a Mesoscopic-Scale Modeling of Their Precipitation. In *Zirconium in the Nuclear Industry: 15th International Symposium* (eds Kammenzind, B. & Limbäck, M.) 29–29–22 (ASTM International, 2009).
365. Thuinet, L., De Backer, A. & Legris, A. Phase-field modeling of precipitate evolution dynamics in elastically inhomogeneous low-symmetry systems: application to hydride precipitation in Zr. *Acta Mater.* **60**, 5311–5321 (2012).
366. Thuinet, L., Legris, A., Zhang, L. & Ambard, A. Mesoscale modeling of coherent zirconium hydride precipitation under an applied stress. *J. Nucl. Mater.* **438**, 32–40 (2013).
367. Shi, S.-Q. & Xiao, Z. A quantitative phase field model for hydride precipitation in zirconium alloys: Part I. Development of quantitative free energy functional. *J. Nucl. Mater.* **459**, 323–329 (2015).
368. Xiao, Z., Hao, M., Guo, X., Tang, G. & Shi, S.-Q. A quantitative phase field model for hydride precipitation in zirconium alloys: Part II. Modeling of temperature dependent hydride precipitation. *J. Nucl. Mater.* **459**, 330–338 (2015).
369. Jokisaari, A. M. & Thornton, K. General method for incorporating CALPHAD free energies of mixing into phase field models: application to the α-zirconium/δ-hydride system. *Calphad* **51**, 334–343 (2015).
370. Bair, J., Zaeem, M. A. & Tonks, M. A phase-field model to study the effects of temperature change on shape evolution of$\char"x03B3$-hydrides in zirconium. *J. Phys. D Appl. Phys.* **49**, 405302 (2016).
371. Bair, J., Asle Zaeem, M. & Schwen, D. Formation path of δ hydrides in zirconium by multiphase field modeling. *Acta Mater.* **123**, 235–244 (2017).
372. Simon, P. C. A. et al. Investigation of δ zirconium hydride morphology in a single crystal using quantitative phase field simulations supported by experiments. *J. Nucl. Mater.* **557**, 153303 (2021).
373. Lin, J. -I & Heuser, B. J. Modeling hydrogen solvus in zirconium solution by the mesoscale phase-field modeling code Hyrax. *Comput. Mater. Sci.* **156**, 224–231 (2019).
374. Welland, M. J. & Hanlon, S. M. Prediction of the zirconium hydride precipitation barrier with an anisotropic 3D phase-field model incorporating bulk thermodynamics and elasticity. *Comput. Mater. Sci.* **171**, 109266 (2020).
375. Shin, W. & Chang, K. Phase-field modeling of hydride reorientation in zirconium cladding materials under applied stress. *Comput. Mater. Sci.* **182**, 109775 (2020).
376. Toghraee, A., Bair, J. & Asle Zaeem, M. Effects of applied load on formation and reorientation of zirconium hydrides: a multiphase field modeling study. *Comput. Mater. Sci.* **192**, 110367 (2021).
377. Wu, S. et al. Phase-field model of hydride blister growth kinetics on zirconium surface. *Front. Mater.* **9**, https://doi.org/10.3389/fmats.2022.916593 (2022).

378. Wei, M. et al. A study of δ-hydride precipitation behavior in Zr alloys by phase-field method. *J. Mater. Res. Technol.* **31**, 2618–2628 (2024).
379. Patel, M., Reali, L., Sutton, A. P., Balint, D. S. & Wenman, M. R. A fast efficient multi-scale approach to modelling the development of hydride microstructures in zirconium alloys. *Comput. Mater. Sci.* **190**, 110279 (2021).
380. Simon, P.-C., Chen, L.-Q., Daymond, M., Tonks, M. & Motta, A. Mechanisms of Mesoscale Hydride Morphology and Reorientation in a Polycrystal Investigated Using Phase-Field Modeling. In *Zirconium in the Nuclear Industry: 20th International Symposium* 807–830 (ASTM International, 2023).
381. Couet, A., Motta, A. T. & Ambard, A. The coupled current charge compensation model for zirconium alloy fuel cladding oxidation: I. Parabolic oxidation of zirconium alloys. *Corros. Sci.* **100**, 73–84 (2015).
382. Courty, O., Motta, A. T. & Hales, J. D. Modeling and simulation of hydrogen behavior in Zircaloy-4 fuel cladding. *J. Nucl. Mater.* **452**, 311–320 (2014).
383. Lebensohn, R. A. & Tomé, C. A self-consistent anisotropic approach for the simulation of plastic deformation and texture development of polycrystals: application to zirconium alloys. *Acta Metall. Mater.* **41**, 2611–2624 (1993).
384. Onimus, F. & Béchade, J.-L. A polycrystalline modeling of the mechanical behavior of neutron irradiated zirconium alloys. *J. Nucl. Mater.* **384**, 163–174 (2009).
385. Erinosho, T. O. & Dunne, F. P. E. Strain localization and failure in irradiated zircaloy with crystal plasticity. *Int. J. Plast.* **71**, 170–194 (2015).
386. Ahn, D.-H., Lee, G.-G., Moon, J., Kim, H. S. & Chun, Y.-B. Analysis of texture and grain shape effects on the yield anisotropy of Zr-2.5wt% Nb pressure tube alloy using crystal plasticity finite element method. *J. Nucl. Mater.* **555**, 153112 (2021).
387. Jose, N. M., Samal, M. K., Durgaprasad, P. V., Alankar, A. & Dutta, B. K. Crystal Plasticity Modelling of Neutron Irradiation Effects on the Flow and Damage Behaviour of Zircaloy-4. In *Advances in Structural Integrity* (eds Jonnalagadda, K., Alankar, A., Balila, N. J. & Bhandakkar, T.) 255-265 (Springer, 2022).
388. Hardie, C., Thomas, R., Liu, Y., Frankel, P. & Dunne, F. Simulation of crystal plasticity in irradiated metals: A case study on Zircaloy-4. *Acta Mater.* **241**, 118361 (2022).
389. Frydrych, K. Modelling irradiation effects in metallic materials using the crystal plasticity theory—a review. *Crystals* **13**, 771 (2023).
390. Zan, X. D. et al. Anisotropic deformation mechanisms of rolling-textured Zircaloy-4 alloy by a crystal plasticity model. *Comput. Mater. Sci.* **229**, 112424 (2023).
391. Patra, A., Tomé, C. N. & Golubov, S. I. Crystal plasticity modeling of irradiation growth in Zircaloy-2. *Philos. Mag.* **97**, 2018–2051 (2017).
392. Ahn, D.-H., Lee, G.-G., Chun, Y.-B. & Jung, J. Y. Prediction of the in-reactor deformation of Zr-2.5wt%Nb pressure tubes using the crystal plasticity finite element method framework. *J. Nucl. Mater.* **570**, 153947 (2022).
393. Roy, R., Long, F. & Daymond, M. R. Evaluation of deformation fields associated with irradiation-induced growth and grain boundary interactions in zirconium. *Materialia* **39**, 102325 (2025).
394. Dupin, N. et al. A thermodynamic database for zirconium alloys. *J. Nucl. Mater.* **275**, 287–295 (1999).
395. Qi, F. et al. Pellet-cladding mechanical interaction analysis of Cr-coated Zircaloy cladding. *Nucl. Eng. Des.* **367**, 110792 (2020).
396. Ma, Z., Shirvan, K., Wu, Y. & Su, G. H. Numerical investigation of ballooning and burst for chromium coated zircaloy cladding. *Nucl. Eng. Des.* **383**, 111420 (2021).
397. Wei, J., Xu, Z., Li, J., Liu, Y. & Wang, B. Crack safety analysis of coating with plastic behavior in surface-coated Zircaloy cladding. *Eng. Fract. Mech.* **280**, 109134 (2023).
398. Capps, N., Mai, A., Kennard, M. & Liu, W. PCI analysis of Zircaloy coated clad under LWR steady state and reactor startup operations using BISON fuel performance code. *Nucl. Eng. Des.* **332**, 383–391 (2018).
399. Dunbar, C. et al. Fuel performance analysis of Cr-coated Zircaloy-4 cladding during a prototypical LOCA event using BISON. *Ann. Nucl. Energy* **200**, 110411 (2024).
400. Aragón, P., Feria, F., Herranz, L. E., Schubert, A. & Van Uffelen, P. Fuel performance modelling of Cr-coated Zircaloy cladding under DBA/LOCA conditions. *Ann. Nucl. Energy* **211**, 110950 (2025).
401. Yang, L., Liu, R., Qiu, C. & Liu, S. Multiphysics analysis of thermal mechanical behavior and tritium migration in FeCrAl and Cr-coated Zircaloy cladding under PWR normal operating and transient conditions. *Prog. Nucl. Energy* **166**, 104942 (2023).
402. Kim, D. & Lee, Y. Diffusion of chromium of Cr-coated Zircaloy accident tolerant fuel cladding: Model development and experimental validation. *Surf. Coat. Technol.* **468**, 129698 (2023).
403. Zhang, W. et al. A crystal plasticity finite element-based model for predicting the fatigue life of Cr-coated Zr4 alloy. *Int. J. Fatigue* **200**, 109091 (2025).
404. Gamble, K. A. et al. An investigation of FeCrAl cladding behavior under normal operating and loss of coolant conditions. *J. Nucl. Mater.* **491**, 55–66 (2017).
405. Sweet, R. T., George, N. M., Maldonado, G. I., Terrani, K. A. & Wirth, B. D. Fuel performance simulation of iron-chrome-aluminum (FeCrAl) cladding during steady-state LWR operation. *Nucl. Eng. Des.* **328**, 10–26 (2018).
406. Liu, R., Zhou, W. & Cai, J. Multiphysics modeling of accident tolerant fuel-cladding U3Si2-FeCrAl performance in a light water reactor. *Nucl. Eng. Des.* **330**, 106–116 (2018).
407. Chen, P. et al. A comparative study of in-pile behaviors of FeCrAl cladding under normal and accident conditions with updated FROBA-ATF code. *Nucl. Eng. Des.* **371**, 110889 (2021).
408. Aragón, P., Feria, F. & Herranz, L. E. Modelling FeCrAl cladding thermo-mechanical performance. Part I: Steady-state conditions. *Prog. Nucl. Energy* **153**, 104417 (2022).
409. Aragón, P., Feria, F. & Herranz, L. E. Modelling FeCrAl cladding thermo-mechanical performance. Part II: comparative analysis with Zircaloy under LOCA conditions. *Prog. Nucl. Energy* **163**, 104838 (2023).
410. Lee, S. K. et al. BISON validation of FeCrAl cladding mechanical failure during simulated reactivity-initiated accident conditions. *J. Nucl. Mater.* **564**, 153676 (2022).
411. Deng, C. et al. Finite element based fuel performance investigation of U3Si2-FeCrAl design under normal and RIA conditions. *Prog. Nucl. Energy* **149**, 104265 (2022).
412. Chang, K. et al. Theory-guided bottom-up design of the FeCrAl alloys as accident tolerant fuel cladding materials. *J. Nucl. Mater.* **516**, 63–72 (2019).
413. Bigdeli, S. et al. Strategies for High-Temperature Corrosion Simulations of Fe-Based Alloys Using the Calphad Approach: Part I. *J. Phase Equilib. Diffus.* **42**, 403–418 (2021).
414. Roy, I. et al. Optimizing chemistry for designing oxidation resistant FeCrAl alloys. *MRS Adv.* **8**, 21–26 (2023).
415. Roy, I. et al. Data-driven predictive modeling of FeCrAl oxidation. *Mater. Lett.: X* **17**, 100183 (2023).
416. Ye, T. et al. Primary radiation damage characteristics in displacement cascades of FeCrAl alloys. *J. Nucl. Mater.* **549**, 152909 (2021).
417. Yao, H. et al. Atomistic observation of defect generation and microstructural evolution in polycrystalline FeCrAl alloys under different irradiation conditions. *Nanomaterials* **15**, 988 (2025).
418. Zhang, J. & Ding, S. Mesoscale simulation research on the homogenized elasto-plastic behavior of FeCrAl alloys. *Mater. Today Commun.* **22**, 100718 (2020).

419. Kumagai, T., Pachaury, Y., Maccione, R., Wharry, J. & El-Azab, A. An atomistic investigation of dislocation velocity in body-centered cubic FeCrAl alloys. *Materialia* **18**, 101165 (2021).
420. Yao, H. et al. Atomic-scale investigation of creep behavior and deformation mechanism in nanocrystalline FeCrAl alloys. *Mater. Des.* **206**, 109766 (2021).
421. Dai, H. et al. Effect of Cr and Al on elastic constants of FeCrAl alloys investigated by molecular dynamics method. *Metals* **12**, 558 (2022).
422. Yao, H. et al. Structural evolution and transitions of mechanisms in creep deformation of nanocrystalline FeCrAl alloys. *Nanomaterials* **13**, 631 (2023).
423. Pachaury, Y., Warren, G., Wharry, J. P., Po, G. & El-Azab, A. Plasticity in irradiated FeCrAl nanopillars investigated using discrete dislocation dynamics. *Int. J. Plast.* **167**, 103676 (2023).
424. Li, C., Chen, S., Du, S., Yu, J. & Zhang, Y. Development of constitutive relationship for thermomechanical processing of FeCrAl alloy to predict hot deformation behavior. *Materials* **18**, 3007 (2025).
425. Wei, Q. et al. Crystal structures, mechanical properties, and electronic structure analysis of ternary FeCrAl alloys. *Phys. Lett. A* **533**, 130228 (2025).
426. Massey, C. P. et al. Microstructure dependent burst behavior of oxide dispersion-strengthened FeCrAl cladding. *Mater. Des.* **234**, 112307 (2023).
427. Sweet, R. T., Pastore, G. & Wirth, B. D. Analysis of FeCrAl cladding performance under loss-of-coolant accident conditions. *Nucl. Eng. Des.* **414**, 112556 (2023).
428. Sweet, R. T., Massey, C. P., Hirschhorn, J. A., Bell, S. B. & Kane, K. A. Wrought FeCrAl alloy (C26M) cladding behavior and burst under simulated loss-of-coolant accident conditions. *Nucl. Eng. Des.* **431**, 113712 (2025).
429. Ravi, S. K. et al. Elucidating precipitation in FeCrAl alloys through explainable AI: a case study. *Comput. Mater. Sci.* **230**, 112440 (2023).
430. Wang, J., Zhang, H., Huang, W. & Lu, Z. Effects of aluminum diffusion on the oxide of the FeCrAl alloys surface: a first-principles study. *Mater. Today Commun.* **33**, 104594 (2022).
431. Wang, J., Yan, K., Huang, W. & Lu, Z. Mechanisms of Al2O3 and Cr2O3 formation during FeCrAl alloy oxidation: a first-principles study. *Appl. Surf. Sci.* **644**, 158782 (2024).
432. Ni, Y. et al. A first-principle study of the effect of yttrium on the oxidation resistance of FeCrAl alloys. *Mater. Technol.* **40**, 2502957 (2025).
433. Kharchenko, D. O. et al. Modeling phase separation and composition patterning in FeCrAl alloys at neutron irradiation. *Phys. Scr.* **99**, 075921 (2024).
434. Deck, C. P., Khalifa, H. E., Sammuli, B., Hilsabeck, T. & Back, C. A. Fabrication of SiC-SiC composites for fuel cladding in advanced reactor designs. *Prog. Nucl. Energy* **57**, 38–45 (2012).
435. Stempien, J. D., Carpenter, D. M., Kohse, G. & Kazimi, M. S. Characteristics of composite silicon carbide fuel cladding after irradiation under simulated PWR conditions. *Nucl. Technol.* **183**, 13–29 (2013).
436. Stone, J. G. et al. Stress analysis and probabilistic assessment of multi-layer SiC-based accident tolerant nuclear fuel cladding. *J. Nucl. Mater.* **466**, 682–697 (2015).
437. Angelici Avincola, V., Guenoun, P. & Shirvan, K. Mechanical performance of SiC three-layer cladding in PWRs. *Nucl. Eng. Des.* **310**, 280–294 (2016).
438. Singh, G. et al. Parametric evaluation of SiC/SiC composite cladding with UO2 fuel for LWR applications: fuel rod interactions and impact of nonuniform power profile in fuel rod. *J. Nucl. Mater.* **499**, 155–167 (2018).
439. Li, W. & Shirvan, K. ABAQUS analysis of the SiC cladding fuel rod behavior under PWR normal operation conditions. *J. Nucl. Mater.* **515**, 14–27 (2019).
440. Wang, H., Liu, S., Li, Y., Li, W. & Wu, J. Modeling of the thermomechanical behavior of braided SiCf/SiC composite cladding tube during irradiation. *J. Nucl. Mater.* **608**, 155723 (2025).
441. Lee, Y., No, H. C. & Lee, J. I. Design optimization of multi-layer Silicon Carbide cladding for light water reactors. *Nucl. Eng. Des.* **311**, 213–223 (2017).
442. Cozzo, C. & Rahman, S. SiC cladding thermal conductivity requirements for normal operation and LOCA conditions. *Prog. Nucl. Energy* **106**, 278–283 (2018).
443. Alabdullah, M. & Ghoniem, N. M. Damage mechanics modeling of the non-linear behavior of SiC/SiC ceramic matrix composite fuel cladding. *J. Nucl. Mater.* **524**, 296–311 (2019).
444. Spilker, K., Lebensohn, R. A., Jacobsen, G. & Capolungo, L. A mean field homogenization model for the mechanical response of ceramic matrix composites. *Compos. Struct.* **352**, 118630 (2025).
445. Maximenko, A., Izhvanov, O. & Olevsky, E. A. Modeling of fuel-cladding stresses in porous UC/SIC fuel pins. *Nucl. Eng. Des.* **359**, 110455 (2020).
446. Kocevski, V., Lopes, D. A., Claisse, A. J. & Besmann, T. M. Understanding the interface interaction between U3Si2 fuel and SiC cladding. *Nat. Commun.* **11**, 2621 (2020).
447. Bonny, G., Buongiorno, L., Bakaev, A. & Castin, N. Models and regressions to describe primary damage in silicon carbide. *Sci. Rep.* **10**, 10483 (2020).
448. Yin, C. et al. A multi-scale simulation study of irradiation swelling of silicon carbide. *Materials* **15**, 3008 (2022).
449. Pan, C. et al. Atomistic simulation of brittle-to-ductile transition in silicon carbide embedded with nano-sized helium bubbles. *J. Phys. D: Appl. Phys.* **56**, 485301 (2023).
450. Rabiee, H., Hassanzadeh, A., Sakhaeinia, H. & Alahyarizadeh, G. Effect of the point defect of silicon carbide cladding on mechanical properties: a molecular-dynamics study. *Chem. Pap.* **78**, 3815–3830 (2024).
451. Kobayashi, K. & Alam, S. B. Physics-regularized neural networks for predictive modeling of silicon carbide swelling with limited experimental data. *Sci. Rep.* **14**, 30666 (2024).
452. Feng, Y. et al. Multiscale modeling of SiCf/SiC nuclear fuel cladding based on FE-simulation of braiding process. *Front. Mater.* **7**, https://doi.org/10.3389/fmats.2020.634112 (2021).
453. Yan, Z. & Fan, X. Study on mechanical properties of SiC_f/SiC nuclear cladding tube based on braiding process simulation and multi-scale FE analysis. *J. Ceram.* **45**, 191–198 (2024).
454. Hu, C., Labuz, J. F., Koyanagi, T. & Le, J.-L. Mechanistic modeling of lifetime distribution of SiC/SiC composite claddings. *J. Am. Ceram. Soc.* **106**, 3066–3077 (2023).
455. Xiao, C. et al. Study on frictional behavior of SiCf/SiC composite clad tube clamping condition under nuclear irradiation. *Friction* **12**, 919–938 (2024).
456. Singh, G., Yu, J., Xu, F., Yao, T. & Xu, P. Multiscale modeling of silicon carbide cladding for nuclear applications: thermal performance modeling. *Energies* **17**, 6124 (2024).
457. Jacobsen, G. M. et al. Multiscale modeling of the mechanical response of silicon carbide composite within the accelerated fuel qualification framework. *Nucl. Technol.* **0**, 1–19 (2025).
458. Xue, J., Wang, S., Chen, Z. & Yang, Z. A multiscale model for the thermomechanical behavior of SiC composite cladding subjected to thermo-mechanical irradiation coupling. *J. Nucl. Mater.* **615**, 155948 (2025).
459. Boltax, A., Murray, P. & Biancheria, A. Fast reactor fuel performance model development. *Nucl. Appl. Technol.* **9**, 326–337 (1970).
460. Kramer, J. M. & Dimelfi, R. J. Modeling deformation and failure of fast reactor cladding during simulated accident transients. *Nucl. Eng. Des.* **63**, 47–54 (1981).
461. Kramer, J. M., Liu, Y. Y., Billone, M. C. & Tsai, H. C. Modeling the behavior of metallic fast reactor fuels during extended transients. *J. Nucl. Mater.* **204**, 203–211 (1993).

462. Sobolev, V., Malambu, E. & Abderrahim, H. A. Design of a fuel element for a lead-cooled fast reactor. *J. Nucl. Mater.* **385**, 392–399 (2009).
463. Karahan, A. Modelling of thermo-mechanical and irradiation behavior of metallic and oxide fuels for sodium fast reactors. Thesis, Massachusetts Institute of Technology. http://dspace.mit.edu/handle/1721.1/57693 (2009).
464. Karahan, A. & Buongiorno, J. A new code for predicting the thermo-mechanical and irradiation behavior of metallic fuels in sodium fast reactors. *J. Nucl. Mater.* **396**, 283–293 (2010).
465. Karahan, A. & Buongiorno, J. Modeling of thermo-mechanical and irradiation behavior of mixed oxide fuel for sodium fast reactors. *J. Nucl. Mater.* **396**, 272–282 (2010).
466. Miao, Y. et al. Metallic fuel cladding degradation model development and evaluation for BISON. *Nucl. Eng. Des.* **385**, 111531 (2021).
467. Ryu, H. J., Kim, Y. S. & Yacout, A. M. Thermal creep modeling of HT9 steel for fast reactor applications. *J. Nucl. Mater.* **409**, 207–213 (2011).
468. Clausen, B., Brown, D. W., Bourke, M. A. M., Saleh, T. A. & Maloy, S. A. In situ neutron diffraction and Elastic-Plastic Self-Consistent polycrystal modeling of HT-9. *J. Nucl. Mater.* **425**, 228–232 (2012).
469. Tallman, A. E. et al. Data-driven constitutive model for the inelastic response of metals: Application to 316h steel. *Integr. Mater. Manuf. Innov.* **9**, 339–357 (2020).
470. Tallman, A. E., Arul Kumar, M., Matthews, C. & Capolungo, L. Surrogate modeling of viscoplasticity in steels: application to thermal, irradiation creep and transient loading in HT-9 cladding. *JOM* **73**, 126–137 (2021).
471. Zhou, F., Hu, C., Zeng, X. & Kang, M. Simulation of steel corrosion and iron yield in LFR with lead coolant. *Energy Rep.* **9**, 243–253 (2023).
472. Wang, G., Wang, Z. & Yun, D. Cladding failure modelling for lead-based fast reactors: a review and prospects. *Metals* **13**, 1524 (2023).
473. Odette, G. R. & Lucas, G. E. Embrittlement of nuclear reactor pressure vessels. *JOM* **53**, 18–22 (2001).
474. Odette, G. & Lucas, G. Irradiation Embrittlement of Reactor Pressure Vessel Steels: Mechanisms, Models, and Data Correlations. In *Radiation Embrittlement of Nuclear Reactor Pressure Vessel Steels: An International Review (Second Volume)* Vol. STP909-EB (ed. Steele, L.) (ASTM International, 1986).
475. Murakami, S., Miyazaki, A. & Mizuno, M. Modeling of irradiation embrittlement of reactor pressure vessel steels. *J. Eng. Mater. Technol.* **122**, 60–66 (1999).
476. Kwon, J., Kwon, S. C. & Hong, J.-H. Prediction of radiation hardening in reactor pressure vessel steel based on a theoretical model. *Ann. Nucl. Energy* **30**, 1549–1559 (2003).
477. Margolin, B. Z. & Kostylev, V. I. Modeling for ductile-to-brittle transition under ductile crack growth for reactor pressure vessel steels. *Int. J. Press. Vessels Pip.* **76**, 309–317 (1999).
478. Margolin, B. Z., Kostylev, V. I., Ilyin, A. V. & Minkin, A. I. Simulation of JR-curves for reactor pressure vessels steels on the basis of a ductile fracture model. *Int. J. Press. Vessels Pip.* **78**, 715–725 (2001).
479. Margolin, B. Z., Kostylev, V. I., Minkin, A. I. & Il'in, A. V. Modeling of ductile crack growth in reactor pressure-vessel steels and determination of JR curves. *Strength Mater.* **34**, 120–130 (2002).
480. Chhibber, R., Singh, H., Arora, N. & Dutta, B. K. Micromechanical modelling of reactor pressure vessel steel. *Mater. Des. (1980-2015)* **36**, 258–274 (2012).
481. Chakraborty, P. & Biner, S. B. A unified cohesive zone approach to model the ductile to brittle transition of fracture toughness in reactor pressure vessel steels. *Eng. Fract. Mech.* **131**, 194–209 (2014).
482. Odette, G. R., Wirth, B. D., Bacon, D. J. & Ghoniem, N. M. Multiscale-multiphysics modeling of radiation-damaged materials: embrittlement of pressure-vessel steels. *MRS Bull.* **26**, 176–181 (2001).
483. Jumel, S. & Van-Duysen, J. C. RPV-1: a virtual test reactor to simulate irradiation effects in light water reactor pressure vessel steels. *J. Nucl. Mater.* **340**, 125–148 (2005).
484. Odette, G. R. & Nanstad, R. K. Predictive reactor pressure vessel steel irradiation embrittlement models: issues and opportunities. *JOM* **61**, 17–23 (2009).
485. Al Mazouzi, A., Alamo, A., Lidbury, D., Moinereau, D. & Van Dyck, S. PERFORM 60: prediction of the effects of radiation for reactor pressure vessel and in-core materials using multi-scale modelling - 60 years foreseen plant lifetime. *Nucl. Eng. Des.* **241**, 3403–3415 (2011).
486. Kwon, J., Mohamed, H. F. M., Kim, Y. M. & Kim, W. Positron annihilation study and computational modeling of defect production in neutron-irradiated reactor pressure vessel steels. *Nucl. Instrum. Methods Phys. Res. Sect. B Beam Interact. Mater.* **262**, 255–260 (2007).
487. Monnet, G., Domain, C., Queyreau, S., Naamane, S. & Devincre, B. Atomic and dislocation dynamics simulations of plastic deformation in reactor pressure vessel steel. *J. Nucl. Mater.* **394**, 174–181 (2009).
488. Bonny, G., Pasianot, R., Castin, N. & Malerba, L. Ternary Fe-Cu-Ni many-body potential to model reactor pressure vessel steels: first validation by simulated thermal annealing. *Philos. Mag.* **89**, 3531–3546 (2009).
489. Zhang, Y., Millett, P. C., Tonks, M. R., Bai, X.-M. & Biner, S. B. Preferential Cu precipitation at extended defects in bcc Fe: an atomistic study. *Comput. Mater. Sci.* **101**, 181–188 (2015).
490. Odette, G. R. & Wirth, B. D. A computational microscopy study of nanostructural evolution in irradiated pressure vessel steels. *J. Nucl. Mater.* **251**, 157–171 (1997).
491. Messina, L., Chiapetto, M., Olsson, P., Becquart, C. S. & Malerba, L. An object kinetic Monte Carlo model for the microstructure evolution of neutron-irradiated reactor pressure vessel steels. *Phys. Status Solidi (a)* **213**, 2974–2980 (2016).
492. Xiong, W. et al. Thermodynamic models of low-temperature Mn-Ni-Si precipitation in reactor pressure vessel steels. *MRS Commun.* **4**, 101–105 (2014).
493. Jacob, A., Domain, C., Adjanor, G., Todeschini, P. & Povoden-Karadeniz, E. Thermodynamic modeling of G-phase and assessment of phase stabilities in reactor pressure vessel steels and cast duplex stainless steels. *J. Nucl. Mater.* **533**, 152091 (2020).
494. Biner, S. B., Rao, W. & Zhang, Y. The stability of precepitates and the role of lattice defects in Fe-1at%Cu-1at%Ni-1at%Mn alloy: a phase-field model study. *J. Nucl. Mater.* **468**, 9–16 (2016).
495. Zhao, Y. Co-precipitated Ni/Mn shell coated nano Cu-rich core structure: a phase-field study. *J. Mater. Res. Technol.* **21**, 546–560 (2022).
496. Yang, W. et al. Dislocation loop assisted precipitation of Cu-rich particles: A phase-field study. *Comput. Mater. Sci.* **228**, 112338 (2023).
497. Ke, H. et al. Thermodynamic and kinetic modeling of Mn-Ni-Si precipitates in low-Cu reactor pressure vessel steels. *Acta Mater.* **138**, 10–26 (2017).
498. Bai, X.-M., Ke, H., Zhang, Y. & Spencer, B. W. Modeling copper precipitation hardening and embrittlement in a dilute Fe-0.3at.% Cu alloy under neutron irradiation. *J. Nucl. Mater.* **495**, 442–454 (2017).
499. Ke, J.-H. & Spencer, B. W. Cluster dynamics modeling of Mn-Ni-Si precipitates coupled with radiation-induced segregation in low-Cu reactor pressure vessel steels. *J. Nucl. Mater.* **569**, 153910 (2022).
500. Monnet, G., Vincent, L. & Gélébart, L. Multiscale modeling of crystal plasticity in reactor pressure vessel steels: prediction of irradiation hardening. *J. Nucl. Mater.* **514**, 128–138 (2019).
501. Shu, S., Wells, P. B., Odette, G. R. & Morgan, D. A kinetic lattice Monte Carlo study of post-irradiation annealing of model reactor pressure vessel steels. *J. Nucl. Mater.* **524**, 312–322 (2019).

502. Mora, D. F., Niffenegger, M., Qian, G., Jaros, M. & Niceno, B. Modelling of reactor pressure vessel subjected to pressurized thermal shock using 3D-XFEM. *Nucl. Eng. Des.* **353**, 110237 (2019).
503. Liu, Y. -c. et al. Machine learning predictions of irradiation embrittlement in reactor pressure vessel steels. *npj Comput. Mater.* **8**, 85 (2022).
504. Liu, Y. -c, Morgan, D., Yamamoto, T. & Odette, G. R. Characterizing the flux effect on the irradiation embrittlement of reactor pressure vessel steels using machine learning. *Acta Mater.* **256**, 119144 (2023).
505. Jacobs, R., Yamamoto, T., Odette, G. R. & Morgan, D. Predictions and uncertainty estimates of reactor pressure vessel steel embrittlement using Machine learning. *Mater. Des.* **236**, 112491 (2023).
506. McMurtrey, M. & Messner, M. *Qualification Challenges for Additive Manufacturing in High Temperature Nuclear Applications* (American Society of Mechanical Engineers Digital Collection, 2021).
507. Mondal, K., Martinez, O. & Jain, P. Advanced manufacturing and digital twin technology for nuclear energy*. *Front. Energy Res*. **12**, https://doi.org/10.3389/fenrg.2024.1339836 (2024).
508. Pitts, S. A. et al. Chapter 14 - Modeling and simulation of advanced manufacturing techniques using MOOSE and MALAMUTE. In *Risk-Informed Methods and Applications in Nuclear and Energy Engineering* (eds Smith, C. L., Le Blanc, K. & Mandelli, D.) 263–286 (Academic Press, 2024).
509. Xie, Z., Jiang, W., Wang, C. & Wu, X. Bayesian inverse uncertainty quantification of a MOOSE-based melt pool model for additive manufacturing using experimental data. *Ann. Nucl. Energy* **165**, 108782 (2022).
510. Yaseen, M., Yushu, D., German, P. & Wu, X. Fast and accurate reduced-order modeling of a MOOSE-based additive manufacturing model with operator learning. *Int. J. Adv. Manuf. Technol.* **129**, 3123–3139 (2023).
511. Roy, A., Swope, A., Devanathan, R. & Van Rooyen, I. J. Chemical composition based machine learning model to predict defect formation in additive manufacturing. *Materialia* **33**, 102041 (2024).
512. Mantri, S. A., Zhang, X. & Chen, W. Y. Influence of post deposition annealing on the microstructural evolution and tensile behavior of austenitic stainless-steel alloy 709 made by laser powder bed fusion. *Mater. Sci. Eng. A* **927**, 148054 (2025).
513. Kadambi, S. B., Schwen, D., Ke, J.-H., He, L. & Jokisaari, A. M. Phase-field modeling of radiation-induced composition redistribution: An application to additively manufactured austenitic Fe-Cr-Ni. *Comput. Mater. Sci.* **255**, 113895 (2025).
514. Hales, J. D. et al. Verification of the BISON fuel performance code. *Ann. Nucl. Energy* **71**, 81–90 (2014).
515. Pastore, G. et al. Uncertainty and sensitivity analysis of fission gas behavior in engineering-scale fuel modeling. *J. Nucl. Mater.* **456**, 398–408 (2015).
516. Bouloré, A. Importance of uncertainty quantification in nuclear fuel behaviour modelling and simulation. *Nucl. Eng. Des.* **355**, 110311 (2019).
517. Tonks, M. R., Bhave, C., Wu, X. & Zhang, Y. 10 - Uncertainty quantification of mesoscale models of porous uranium dioxide. In *Uncertainty Quantification in Multiscale Materials Modeling*, Elsevier Series in Mechanics of Advanced Materials (eds Wang, Y. & McDowell, D. L.) 329–354 (Woodhead Publishing, 2020).
518. Fish, J., Wagner, G. J. & Keten, S. Mesoscopic and multiscale modelling in materials. *Nat. Mater.* **20**, 774–786 (2021).
519. Rempe, J. L. et al. Advanced in-pile instrumentation for materials testing reactors. *IEEE Trans. Nucl. Sci.* **61**, 1984–1994 (2014).
520. Patnaik, S., Lopes, D. A., Besmann, T. M., Spencer, B. W. & Knight, T. W. Experimental system for studying temperature gradient-driven fracture of oxide nuclear fuel out of reactor. *Rev. Sci. Instrum.* **91**, 035101 (2020).
521. Mengyan, H., Xueyan, Z., Cuiting, P., Yixuan, Z. & Jun, Y. Current status of digital twin architecture and application in nuclear energy field. *Ann. Nucl. Energy* **202**, 110491 (2024).
522. Chen, M. et al. Development of the environmental assisted fatigue assessment method for nuclear plants in digital twin. *Nucl. Eng. Technol.* **57**, 103402 (2025).
523. Stewart, R. et al. The AGN-201 Digital Twin: a test bed for remotely monitoring nuclear reactors. *Ann. Nucl. Energy* **213**, 111041 (2025).
524. Yacout, A. M. et al. Fipd: the SFR metallic fuels irradiation & physics database. *Nucl. Eng. Des.* **380**, 111225 (2021).
525. Fuel Experimental Data—IAEA Data Platform. https://data.iaea.org/pages/the-iaea-fuel-database.
526. Advanced Material Database—IAEA Data Platform. https://data.iaea.org/pages/advanced-material-database.
527. Gain Databases. https://gain.inl.gov/resources/databases/.

Acknowledgements

The authors would like to thank Andrea Jokisaari for preliminary planning and discussions regarding this work. Los Alamos National Laboratory, an affirmative action/equal opportunity employer, is operated by Triad National Security, LLC, for the National Nuclear Security Administration of the U.S. Department of Energy under contract number 89233218CNA000001. M.R.T. and A.A. were supported by the University of Florida. D.A.A. was supported by the Nuclear Energy Advanced Modeling and Simulation (NEAMS) program under the U.S. Department of Energy, Office of Nuclear Energy, United States. The funding agencies played no role in the research, planning, or writing of this review.

Author contributions

M.R.T. wrote the first draft of the manuscript and figures. D.A.A. and A.A. revised the manuscript and added additional text. M.R.T., D.A.A., and A.A. reviewed the manuscript.

Competing interests

The authors declare no competing interests.

Additional information

Correspondence and requests for materials should be addressed to Michael R. Tonks.